

University of New Mexico

UNM Digital Repository

Mathematics & Statistics ETDs

Electronic Theses and Dissertations

Summer 6-30-2020

An a posteriori error analysis of stationary incompressible magnetohydrodynamics

Ari E. Rappaport

Follow this and additional works at: https://digitalrepository.unm.edu/math_etds



Part of the [Applied Mathematics Commons](#), and the [Mathematics Commons](#)

Recommended Citation

Rappaport, Ari E.. "An a posteriori error analysis of stationary incompressible magnetohydrodynamics." (2020). https://digitalrepository.unm.edu/math_etds/150

This Thesis is brought to you for free and open access by the Electronic Theses and Dissertations at UNM Digital Repository. It has been accepted for inclusion in Mathematics & Statistics ETDs by an authorized administrator of UNM Digital Repository. For more information, please contact disc@unm.edu.

Ari Rappaport

Candidate

Mathematics and Statistics

Department

This thesis is approved, and it is acceptable in quality and form for publication:

Approved by the Thesis Committee:

Jehanzeb Chaudhry

Chairperson

John Shadid

Member

Deborah Sulsky

Member

**An *a posteriori* error analysis of
stationary incompressible
magnetohydrodynamics**

by

Ari Rappaport

B.S., Mathematics, University of New Mexico, 2018

THESIS

Submitted in Partial Fulfillment of the
Requirements for the Degree of

Master of Science
Mathematics

The University of New Mexico

Albuquerque, New Mexico

July, 2020

Dedication

Dedicated to my girlfriend, my family, and my friends.

Acknowledgments

I would first like to thank my thesis advisors, Professor Jehanzeb Chaudhry and Professor John Shadid. I could not have completed this work without their unfailing support and guidance. I would also like to thank Professor Deborah Sulsky for serving on my thesis committee. Finally, I would like to thank Doctor Tim Wildey for his feedback and suggestions on this research.

An *a posteriori* error analysis of stationary incompressible magnetohydrodynamics

by

Ari Rappaport

B.S., Mathematics, University of New Mexico, 2018

M.S., Mathematics, University of New Mexico, 2020

Abstract

Adjoint based *a posteriori* error analysis is a technique to produce exact error representations for quantities of interests that are functions of the solution of systems of partial differential equations (PDE). The tools used in the analysis consist of duality arguments and compatible residuals. In this thesis we apply *a posteriori* error analysis to the magnetohydrodynamics (MHD) equations. MHD provides a continuum level description of conducting fluids in the presence of electromagnetic fields. The MHD system is therefore a multi-physics system, capturing both fluid and electromagnetic effects. Mathematically, The equations of MHD are highly nonlinear and fully coupled, adding to the complexity of the *a posteriori* analysis. Additionally, there is a stabilization necessary to ensure the so called solenoidal constraint ($\operatorname{div} \mathbf{B} = 0$) is satisfied in a weak sense. We present the new linearized adjoint system, demonstrate its effectiveness on several numerical examples, and prove its well-posedness.

Contents

List of Figures	ix
List of Tables	x
Glossary	xiii
1 Introduction	1
2 Adjoint based analysis for linear problems	4
2.1 Abstract linear problems	5
2.2 Coupled PDE system example	6
2.3 Computing the system adjoint	6
2.4 Weak adjoint definition	7
3 Adjoint based analysis for nonlinear problems	9
3.1 Theoretical foundations	10
3.2 Adjoint based analysis for the nonlinear viscous Burgers equation . .	19

Contents

3.2.1	Numerical experiment for Burgers equation	21
3.3	Adjoint analysis for nonlinearity and Neumann boundary conditions .	22
3.3.1	Numerical experiment for Neumann BCs	24
3.3.2	Vanishing boundary conditions	25
3.4	Adjoint based analysis for the incompressible Navier-Stokes equations	26
4	Adjoint based analysis for MHD	30
4.1	Exact penalty formulation and discretization for incompressible MHD	31
4.1.1	The MHD equations	31
4.1.2	Function spaces for the MHD system	32
4.1.3	Exact penalty formulation	32
4.1.4	Finite element method	33
4.1.5	Quantity of interest (QoI)	34
4.2	Abstract <i>a posteriori</i> error analysis	34
4.3	<i>A posteriori</i> error estimate applied to MHD	37
4.3.1	Weak form of adjoint for incompressible MHD	38
4.3.2	Error representation	39
4.3.3	Non-homogeneous boundary conditions for the MHD system .	40
4.3.4	Error estimate and contributions	41
4.4	Numerical Experiments	42
4.4.1	Hartmann flow in 2D	42

Contents

4.4.2	Magnetic Lid Driven Cavity	45
4.5	Well posedness and derivation of the weak adjoint problem	52
4.5.1	Derivation of the weak form of the adjoint	52
4.5.2	Well posedness of the adjoint problem	55
5	Conclusions and future directions	61
A	Standard function spaces	70
B	Vector identities	72
C	Useful inequalities	74

List of Figures

3.1	A sample 10×10 triangulation for the unit square, \mathcal{T}_h	25
4.1	Plots of the $\ \mathbf{u}\ _{\mathbb{R}^d}$ for the lid driven cavity §4.4.2 using a normalization on the lid velocity over a variety of magnetic Reynolds numbers, Re_m . The other nondimensionalized parameters are $\text{Re} = 5000, \kappa = 1$ for all of these plots.	46
4.2	Demonstrating the homotopy parameter strategy to achieve high fluid Reynolds numbers as described in §4.4.2. The other nondimensionalized parameters $\text{Re}_m = 5.0, \kappa = 1$ for all of these plots. The top row is colored according the b_y and with the arrows representing the vector \mathbf{b} . The bottom row is colored according to the magnitude of \mathbf{u} , with added streamlines.	47

List of Tables

3.1	Effectivity ratios (3.21) for the problem outlined in §3.2 using the error estimate (3.20). The true QoI is exactly $\frac{2}{\pi}$ in this case.	22
3.2	Effectivity ratios (3.21) for the problem outlined in §3.3 using the error estimate (3.31).	25
4.1	Mapping between the abstract framework in §4.2 and the MHD equation in §4.3. \mathcal{N}_{EP} is given in (4.19), $N_{EP,i}$ in (4.20), a_{EP} in (4.21) and $\overline{\mathcal{Z}}_{\mathbf{u}}^*$, $\overline{\mathcal{Z}}_{\mathbf{b}}^*$, $\overline{\mathcal{Y}}^*$, $\overline{\mathcal{C}}^*$ are given in (4.22).	38
4.2	Error in $(u_x, \mathbb{1}_{\Omega_c})$ for the Hartmann problem §4.4.1, with $\mathbb{1}_{\Omega_c} = [-\frac{1}{4}, \frac{1}{2}] \times [-\frac{1}{4}, \frac{1}{4}]$. The finite dimensional space here is $(\mathbb{P}^2, \mathbb{P}^1, \mathbb{P}^1)$ for $(\mathbf{u}, \mathbf{b}, p)$	44
4.3	Error in $(u_x, \mathbb{1}_{\Omega_c})$ for the Hartmann problem §4.4.1. The finite dimensional space here is $(\mathbb{P}^2, \mathbb{P}^2, \mathbb{P}^1)$ for $(\mathbf{u}, \mathbf{b}, p)$	44

List of Tables

4.4 Error in $(u_x, \mathbb{1}_{\Omega_c})$ for the Hartmann problem §4.4.1. The finite dimensional space here is $(\mathbb{P}^3, \mathbb{P}^2, \mathbb{P}^2)$ for $(\mathbf{u}, \mathbf{b}, p)$. Here, we approximate the true solution with the computed solution which results in linearization error as described in Remark 3.1.1. For this accurate a solution, this deteriorates the quality of the estimate which in turn results in a effectivity further from 1. This is confirmed in Table 4.5 where we use the true solution and the effectivity is again close to 1. 45

4.5 Error in $(u_x, \mathbb{1}_{\Omega_c})$ for the Hartmann problem, §4.4.1. The finite dimensional space here is $(\mathbb{P}^3, \mathbb{P}^2, \mathbb{P}^2)$ for $(\mathbf{u}, \mathbf{b}, p)$. No linearization error is present here because we use the true solution in the definition of the adjoint. 45

4.6 error in $(u_x, \mathbb{1}_{\Omega_c})$ for the lid driven cavity §4.4.2. The finite dimensional space here is $(\mathbb{P}^2, \mathbb{P}^1, \mathbb{P}^1)$ for $(\mathbf{u}, \mathbf{b}, p)$. We use an overkill solution on a $400 \times 400 = 160000$ element mesh and $(\mathbb{P}^3, \mathbb{P}^2, \mathbb{P}^2)$ elements. The parameters are $\text{Re} = 1000, \text{Re}_m = 0.4, \kappa = 1$ 48

4.7 Error in $(u_x, \mathbb{1}_{\Omega_c})$ for the lid driven cavity §4.4.2. The finite dimensional space here is $(\mathbb{P}^2, \mathbb{P}^2, \mathbb{P}^1)$ for $(\mathbf{u}, \mathbf{b}, p)$. We use an overkill solution on a $400 \times 400 = 160000$ element mesh and $(\mathbb{P}^3, \mathbb{P}^2, \mathbb{P}^2)$ elements. The parameters are $\text{Re} = 1000, \text{Re}_m = 0.4, \kappa = 1$ 49

4.8 Error in $(u_x, \mathbb{1}_{\Omega_c})$ for the lid driven cavity §4.4.2. The finite dimensional space here is $(\mathbb{P}^2, \mathbb{P}^1, \mathbb{P}^1)$ for $(\mathbf{u}, \mathbf{b}, p)$. We use an overkill solution on a $400 \times 400 = 160000$ element mesh and $(\mathbb{P}^3, \mathbb{P}^2, \mathbb{P}^2)$ elements. The parameters are $\text{Re} = 2000, \text{Re}_m = 0.4, \kappa = 1$ 49

List of Tables

4.9 Error in $(u_x, \mathbb{1}_{\Omega_c})$ for the lid driven cavity §4.4.2. The finite dimensional space here is $(\mathbb{P}^2, \mathbb{P}^2, \mathbb{P}^1)$ for $(\mathbf{u}, \mathbf{b}, p)$. We use an overkill solution on a $400 \times 400 = 160000$ element mesh and $(\mathbb{P}^3, \mathbb{P}^2, \mathbb{P}^2)$ elements. The parameters are $\text{Re} = 2000, \text{Re}_m = 0.4, \kappa = 1$ 49

4.10 Error estimates for $(b_y, \mathbb{1}_{\Omega_c})$ for the lid driven cavity §4.4.2. The finite dimensional space here is $(\mathbb{P}^2, \mathbb{P}^1, \mathbb{P}^1)$ for $(\mathbf{u}, \mathbf{b}, p)$. We use an overkill solution on a $400 \times 400 = 160000$ element mesh and $(\mathbb{P}^3, \mathbb{P}^2, \mathbb{P}^2)$ elements. The parameters are $\text{Re} = 1000, \text{Re}_m = 0.4, \kappa = 1$ 51

4.11 Error estimates for in $(b_y, \mathbb{1}_{\Omega_c})$ for the lid driven cavity §4.4.2. The finite dimensional space here is $(\mathbb{P}^3, \mathbb{P}^1, \mathbb{P}^2)$ for $(\mathbf{u}, \mathbf{b}, p)$. We use an overkill solution on a $400 \times 400 = 160000$ element mesh and $(\mathbb{P}^3, \mathbb{P}^2, \mathbb{P}^2)$ elements. The parameters are $\text{Re} = 1000, \text{Re}_m = 0.4, \kappa = 1$ 51

4.12 Error estimates for $(b_y, \mathbb{1}_{\Omega_c})$ for the lid driven cavity §4.4.2. The finite dimensional space here is $(\mathbb{P}^2, \mathbb{P}^1, \mathbb{P}^1)$ for $(\mathbf{u}, \mathbf{b}, p)$. We use an overkill solution on a $400 \times 400 = 160000$ element mesh and $(\mathbb{P}^3, \mathbb{P}^2, \mathbb{P}^2)$ elements. The parameters are $\text{Re} = 2000, \text{Re}_m = 0.4, \kappa = 1$ 51

4.13 Error estimates for $(b_y, \mathbb{1}_{\Omega_c})$ for the lid driven cavity §4.4.2. The finite dimensional space here is $(\mathbb{P}^3, \mathbb{P}^1, \mathbb{P}^2)$ for $(\mathbf{u}, \mathbf{b}, p)$. We use an overkill solution on a $400 \times 400 = 160000$ element mesh and $(\mathbb{P}^3, \mathbb{P}^2, \mathbb{P}^2)$ elements. The parameters are $\text{Re} = 2000, \text{Re}_m = 0.4, \kappa = 1$ 52

Glossary

$\Omega \subset \mathbb{R}^d$, $d = 2, 3$, is a Lipschitz domain

$$L^p(\Omega) := \left\{ v : \Omega \rightarrow \mathbb{R} \mid \left(\int_{\Omega} v^p dx \right)^{1/p} < \infty \right\}$$

$(u, v)_S := \int_S u v dx$ is the L^2 inner over $S \subset \overline{\Omega}$

$(u, v) := \int_{\Omega} u v dx$ by default over Ω

$$\|v\| := \sqrt{(v, v)}$$

$$\mathbf{L}^p(\Omega) := \{ \mathbf{v} : \Omega \rightarrow \mathbb{R}^d \mid v_i \in L^p(\Omega), \forall i = 1, \dots, d \}$$

$$(\mathbf{u}, \mathbf{v}) := \int_{\Omega} \mathbf{u}^T \mathbf{v} dx = \sum_{i=1}^d (u_i, v_i)$$

$$\|v\|_m := \left(\sum_{|\alpha|=0}^m \|D^{\alpha} v\|^2 \right)^{1/2}. \text{ where } \alpha = (\alpha_1, \dots, \alpha_m) \text{ and } D^{\alpha} v := \partial_{x_1}^{\alpha_1} \dots \partial_{x_m}^{\alpha_m} v$$

$$H^m(\Omega) := \{ v : \Omega \rightarrow \mathbb{R} \mid \|v\|_m < \infty \}.$$

$$\mathbf{H}^m(\Omega) := \{ \mathbf{v} : \Omega \rightarrow \mathbb{R}^d \mid v_i \in H^m(\Omega), i = 1, \dots, d \}.$$

$$\mathbf{H}(\text{curl}, \Omega) := \{ \mathbf{v} \in \mathbf{L}^2(\Omega) \mid \nabla \times \mathbf{v} \in \mathbf{L}^2(\Omega) \}$$

$$\mathbf{H}(\text{div}, \Omega) := \{ \mathbf{v} \in \mathbf{L}^2(\Omega) \mid \nabla \cdot \mathbf{v} \in L^2(\Omega) \}$$

$H_0^1(\Omega) := \{ v \in H^1(\Omega) \mid \gamma v = 0 \}$ where $\gamma : \Omega \rightarrow \partial\Omega$ is the trace operator

$$\nabla \mathbf{u} := \left[\nabla u_1, \dots, \nabla u_d \right]^T$$

Glossary

$$\nabla \mathbf{u} : \nabla \mathbf{v} = \sum_{i=1}^d \nabla u_i \cdot \nabla v_i$$

$$(\mathbf{u} \cdot \nabla) \mathbf{v} = (\nabla \mathbf{v}) \mathbf{u}$$

$$\Delta \mathbf{u} = [\Delta u_1, \dots, \Delta u_d]^T$$

$\stackrel{(\cdot)}{=}$ and $\stackrel{(\cdot)}{\leq}$ denote that the equality or inequality is justified by equation (\cdot)

Chapter 1

Introduction

The resistive magnetohydrodynamics (MHD) equations provide a continuum model for conducting fluids subject to magnetic fields and are often used to model important applications e.g. higher-density, highly collisional plasmas. In this context, MHD calculations aid physicists in understanding both thermonuclear fusion and astrophysical plasmas as well as understanding the behavior of liquid metals [38, 59]. From a phenomenological perspective, the governing equations of MHD couple Navier-Stokes equations for fluid dynamics with a reduced set of Maxwell's equations for low frequency electromagnetic phenomenon. Structurally, the equations of MHD form a highly coupled, nonlinear, non self-adjoint system of partial differential equations (PDEs). Analytical solutions to the MHD system cannot be obtained for practical configurations; instead numerical solutions are sought. Finite element formulations of incompressible resistive MHD include stabilization methods based on variational multiscale (VMS) approaches [45, 46, 58], exact and weighted penalty methods [39, 35, 54, 51], first order system least squares (FOSLS) [1, 3, 2, 41] and structure preserving methods [53, 34, 42, 11, 52]. In this thesis we restrict ourselves to the stationary MHD equations based on the exact penalty finite element formulation, originally developed in [39] from a finite element method discretization. We

Chapter 1. Introduction

do not employ specialized solver strategies e.g. block preconditioning as the problem size we consider does not merit it.

The numerical solution of complex equations like the MHD equations often have a significant discretization error for solution with significant fine scale spatial structures. This error must be quantified for the reliable use of MHD equations in numerous science and engineering fields. Accurate error estimation is a key component of predictive computational science and uncertainty quantification [31, 29, 18]. Moreover, the error depends on a complex interaction between many contributions. Thus, the availability of an accurate error estimate and the different sources of error also offers the potential of optimizing the choice of discretization parameters in order to achieve desired accuracy in an efficient fashion. In this work we leverage adjoint based *a posteriori* error estimates for a quantity of interest (QoI) related to the solution of the MHD equations. These estimates provide a concrete error analysis of different contributions of error, as well as inform solver and discretization strategies.

In many scientific and engineering applications, the goal of running a simulation is to compute a set of specific QoIs of the solution, for example the drag over a plane wing in a compressible CFD context. Adjoint based analysis [36, 10, 32, 24, 5, 8] for estimating the error in a numerically computed QoI has found success for a wide variety of numerical methods and discretizations ranging from finite element [15, 31, 33], finite difference [20], finite volume [17, 9], time integration [32, 19, 20, 16], operator splitting techniques [31, 33] and uncertainty quantification [28, 30, 18].

Adjoint based *a posteriori* error analysis uses variational analysis and duality to relate errors to computable residuals. In particular, one solves an adjoint problem whose solution provides the residual weighting to produce the error in the QoI. The technique also naturally allows to identify and isolate different components of error arising from different aspects of discretization and solution methods, by analyzing different components of the weighted residual separately.

Chapter 1. Introduction

This thesis is organized as follows. We will first introduce the basic ideas of ABAPEA for linear problems in Chapter 2. Next, Chapter 3 is devoted to ABAPEA for nonlinear problems. We first summarize necessary theory from nonlinear functional analysis in §3.1. This naturally leads into ABAPEA for representative nonlinear problems starting with §3.2. Finally, the original contributions of this work are concentrated in Chapter 4. Here, we apply ABAPEA to the equations of resistive, incompressible MHD, along with supporting numerical results, and a well-posedness proof for the resulting weak adjoint problem. Finally, in Chapter 5, we present some conclusions about this work, as well as possible directions for further research in this area.

Chapter 2

Adjoint based analysis for linear problems

In this chapter we introduce the ideas of adjoint based *a posteriori* error analysis (ABAPEA) in an abstract setting for linear problems [25, 32]. We give a concrete example for a system of convection diffusion equations, as well as the corresponding error representation.

Let V be a Hilbert space $\langle\langle \cdot, \cdot \rangle\rangle$ denote the inner product on V . Next let $L : V \rightarrow V$ be a linear operator. Suppose we have the following abstract boundary value problem (BVP): find $u \in V$ such that

$$\begin{aligned} Lu &= f, & \text{in } \Omega, \\ u &= 0, & \text{on } \partial\Omega. \end{aligned} \tag{2.1}$$

This problem can represent a wide range of linear boundary value problems e.g. $L(v) = -\Delta v$ for the Poisson equation, $L(v) = -\nabla \cdot (K \nabla v) + \mathbf{b} \cdot \nabla v$ for convection diffusion with diffusivity K and transport velocity \mathbf{b} etc.

Exact solutions to (2.1) are often difficult or infeasible to obtain. Instead, one often seeks an approximate solution $u_h \in V_h \subset V$, where V_h is a finite dimension sub-

space of V whose dimension depends on the parameter h . With such an approximate solution it is natural to ask questions about the so called error, $u - u_h$ and functions thereof. Indeed, frequently the goal of obtaining the solution u of (2.1) is not to know $u(x)$ for all $x \in \Omega$, but rather to compute a quantity of interest $\mathcal{Q}(u) = \langle\langle u, \psi \rangle\rangle$. We now proceed to study the error in such a quantity of interest $\mathcal{Q}(u - u_h) = \langle\langle u - u_h, \psi \rangle\rangle$ where $\psi \in V$.

2.1 Abstract linear problems

The following definition is crucial for the analysis.

Definition 2.1.1. *The adjoint to L , denoted L^* , is the unique linear operator $L^* : V \rightarrow V$ defined by*

$$\langle\langle Lu, v \rangle\rangle = \langle\langle u, L^*v \rangle\rangle, \quad \forall u, v \in V. \quad (2.2)$$

We now consider the associated adjoint problem: find $\phi \in V^*$ such that

$$\begin{aligned} L^*\phi &= \psi, & \text{in } \Omega, \\ \phi &= 0, & \text{on } \partial\Omega. \end{aligned} \quad (2.3)$$

Now we present the following error representation,

Theorem 2.1.1. *The error in the QoI $\mathcal{Q}(u - u_h) = \langle\langle u - u_h, \psi \rangle\rangle$ is compatible as*

$$\langle\langle u - u_h, \psi \rangle\rangle = \langle\langle f, \phi \rangle\rangle - \langle\langle Lu_h, \phi \rangle\rangle. \quad (2.4)$$

Proof. We have that

$$\langle\langle u - u_h, \psi \rangle\rangle = \langle\langle u - u_h, L^*\phi \rangle\rangle = \langle\langle Lu - Lu_h, \phi \rangle\rangle = \langle\langle f, \phi \rangle\rangle - \langle\langle Lu_h, \phi \rangle\rangle. \quad (2.5)$$

□

We now present an example of the abstract analysis to a coupled system of PDE.

2.2 Coupled PDE system example

We first consider the following problem: find $\mathbf{u} := [u_1, u_2]^T$ such that

$$\begin{aligned} \nabla^2 u_1 + \mathbf{b}_1 \cdot \nabla u_2 &= 0, & \text{in } \Omega, \\ \nabla^2 u_2 + \mathbf{b}_2 \cdot \nabla u_1 &= 0, & \text{in } \Omega, \\ \mathbf{u} &= 0, & \text{on } \partial\Omega. \end{aligned} \tag{2.6}$$

where $\mathbf{b}_i = \mathbf{b}_i(x)$ depends only on $x \in \Omega$. We will see another example of a coupled system in Chapter 4, namely the MHD equations.

2.3 Computing the system adjoint

First let $\mathscr{W} := H_0^1(\Omega) \times H_0^1(\Omega)$ be a product Hilbert space. Integrating, combining equations, and performing integration by parts, the weak problem associated with (2.6) is: find $\mathbf{u} \in \mathscr{W}$ such that

$$-(\nabla u_1, \nabla v_1) + (\mathbf{b}_1 \cdot \nabla u_2, v_1) - (\nabla u_2, \nabla v_2) + (\mathbf{b}_2 \cdot \nabla u_1, v_2) = 0, \quad \forall \mathbf{v} \in \mathscr{W}. \tag{2.7}$$

We now employ (B.4) and the divergence theorem to compute the formal adjoint of the weak primal problem (2.7),

$$\begin{aligned} a(u, v) &= -(\nabla u_1, \nabla v_1) + (\mathbf{b}_1 \cdot \nabla u_2, v_1) - (\nabla u_2, \nabla v_2) + (\mathbf{b}_2 \cdot \nabla u_1, v_2) \\ &= -(\nabla u_1, \nabla v_1) - (u_2, \nabla \cdot (v_1 \mathbf{b}_1)) - (\nabla u_2, \nabla v_2) - (u_1, \nabla \cdot (v_2 \mathbf{b}_2)) \\ &= (u_1, \nabla^2 v_1) - (u_2, \nabla \cdot (v_1 \mathbf{b}_1)) + (u_2, \nabla^2 v_2) - (u_1, \nabla \cdot (v_2 \mathbf{b}_2)). \end{aligned}$$

We see that (2.2) is now satisfied since all operators have been moved off of \mathbf{u} . Thus following (2.3), the strong adjoint problem should be: find ϕ such that

$$\begin{aligned} \nabla^2 \phi_1 - \nabla \cdot (\phi_2 \mathbf{b}_2) &= \psi_1, & \text{in } \Omega, \\ -\nabla \cdot (\mathbf{b}_1 \phi_1) + \nabla^2 \phi_2 &= \psi_2, & \text{in } \Omega, \\ \phi &= \mathbf{0}, & \text{on } \partial\Omega. \end{aligned} \tag{2.8}$$

The corresponding weak adjoint problem to (2.8) is: find $\phi \in \mathcal{W}$ such that

$$-(\nabla\phi_1, \nabla v_1) - (\phi_2, \mathbf{b}_1 \cdot \nabla v_1) + (\nabla\phi_2, \nabla v_2) - (\phi_1, \mathbf{b}_2 \cdot \nabla v_2) = (\boldsymbol{\psi}, \mathbf{v}), \quad \forall \mathbf{v} \in \mathcal{W}. \quad (2.9)$$

2.4 Weak adjoint definition

One can also carry out ABAPEA at the level of bilinear forms. Given a bilinear form $a : V \times V \rightarrow \mathbb{R}$ (e.g. $a(u, v) = (\nabla u, \nabla v)$), the adjoint bilinear form $a^* : V \times V \rightarrow \mathbb{R}$ is defined by the relation [36, 10]

$$a^*(w, v) = a(v, w), \quad \forall w, v \in V. \quad (2.10)$$

If ϕ solves the dual problem: find $\phi \in V$ such that

$$a^*(\phi, v) = \langle\langle \boldsymbol{\psi}, v \rangle\rangle, \quad \forall v \in V,$$

then we have the following error representation,

Theorem 2.4.1. *The error in a (linear) QoI represented by $QoI = \langle\langle \boldsymbol{\psi}, e \rangle\rangle$ is compatible as $\langle\langle \boldsymbol{\psi}, e \rangle\rangle = \langle\langle f, \phi \rangle\rangle - a(u_h, \phi)$.*

Proof. The proof follows in the same way as for the strong adjoint,

$$\langle\langle \boldsymbol{\psi}, e \rangle\rangle = a^*(\phi, e) = a(e, \phi) = a(u, \phi) - a(u_h, \phi) = \langle\langle f, \phi \rangle\rangle - a(u_h, \phi). \quad (2.11)$$

□

For the convection diffusion example of the previous section, the primal bilinear form is given by the LHS of (2.7) and the weak adjoint form is given by the LHS of (2.9). The error representation $\langle\langle \boldsymbol{\psi}, e \rangle\rangle$ is given, for an arbitrary finite dimensional

Chapter 2. Adjoint based analysis for linear problems

approximation $\mathbf{u}_h = \begin{bmatrix} u_{1h}, u_{2h} \end{bmatrix}^T$, by

$$\begin{aligned}
 (\boldsymbol{\psi}, \mathbf{e}) &= -(\nabla\phi_1, \nabla e_1) - (\phi_2, \mathbf{b}_1 \cdot \nabla e_1) + (\nabla\phi_2, \nabla e_2) - (\phi_1, \mathbf{b}_2 \cdot \nabla e_2) \\
 &= -(\nabla e_1, \nabla\phi_1) + (\mathbf{b}_1 \cdot \nabla e_2, \phi_1) - (\nabla e_2, \nabla\phi_2) + (\mathbf{b}_2 \cdot \nabla e_1, \phi_2) \\
 &= -(\nabla u_1, \nabla\phi_1) + (\mathbf{b}_1 \cdot \nabla u_2, \phi_1) - (\nabla u_2, \nabla\phi_2) + (\mathbf{b}_2 \cdot \nabla u_1, \phi_2) \\
 &\quad - (-(\nabla u_{1h}, \nabla\phi_1) + (\mathbf{b}_1 \cdot \nabla u_{2h}, \phi_1) - (\nabla u_{2h}, \nabla\phi_2) + (\mathbf{b}_2 \cdot \nabla u_{1h}, \phi_2)) \\
 &= (\mathbf{f}, \boldsymbol{\phi}) - (-(\nabla u_{1h}, \nabla\phi_1) + (\mathbf{b}_1 \cdot \nabla u_{2h}, \phi_1) - (\nabla u_{2h}, \nabla\phi_2) + (\mathbf{b}_2 \cdot \nabla u_{1h}, \phi_2)).
 \end{aligned}$$

Note the abstract inner product $\langle\langle \cdot, \cdot \rangle\rangle$ is represented here by the \mathbf{L}^2 inner product. This viewpoint will be important in Chapter 4 where we define an adjoint for the exact penalty weak form.

Chapter 3

Adjoint based analysis for nonlinear problems

To motivate the nonlinear adjoint analysis, consider the following scalar problem, find $u \in H^2(\Omega)$ such that

$$\begin{aligned}\nabla^2 u + \mathbf{b} \cdot \nabla u + u^2 &= 0, && \text{in } \Omega, \\ u &= 0, && \text{on } \partial\Omega.\end{aligned}$$

We consider the associated operator,

$$F(u) = \nabla^2 u - \mathbf{b} \cdot \nabla u + u^2.$$

The path for defining the adjoint to a nonlinear operator is not as straightforward as in the case of a linear operator. Suppose we are solving the linear equation, $Lu = b$, and we obtain a computed solution u_h . Since L is linear, $Le = L(u - u_h) = Lu - Lu_h = b - Lu_h$. Thus, we seek a linearized operator (about the error), \bar{F} such that

$$\bar{F}e = F(u) - F(u_h). \tag{3.1}$$

First however, we will need to develop some ideas about differentiation in Banach spaces. [7].

3.1 Theoretical foundations

For the rest of the section, assume that X and Y are Banach spaces with norms $\|\cdot\|_X, \|\cdot\|_Y$ where we will sometimes drop the subscript if it is clear from context. We begin by defining a generalization of the gradient on \mathbb{R}^d to Banach spaces.

Definition 3.1.1. *Let $F : X \rightarrow Y$ be any map. Given $x \in X$ we say that F is Fréchet differentiable (or simply differentiable) at x if there is a bounded linear map $L : X \rightarrow Y$ such that*

$$\lim_{h \rightarrow 0} \frac{\|F(x+h) - F(x) - Lh\|_Y}{\|h\|_X} = 0.$$

We call the operator L the Fréchet derivative of F at x and denote it by $L = F'(x)$. Our first task will be to prove the Fréchet derivative is unique.

Proposition 3.1.1. *Given $x \in X$, the derivative $F'(x) : X \rightarrow Y$ is unique.*

Proof. Suppose the contrary, that there is another linear map \hat{L} satisfying Definition 3.1.1 with $F'(x) \neq \hat{L}$ as operators. From the definition, for any $h \in X$, we should have

$$\frac{\|F'(x)h - \hat{L}h\|}{\|h\|} \rightarrow 0 \text{ as } \|h\| \rightarrow 0. \quad (3.2)$$

Since we assume $F'(x) \neq \hat{L}$ there exists $h^* \in X$ such that $a := \|F'(x)h^* - \hat{L}h^*\| \neq 0$. Taking $h = th^*$ for $t \in \mathbb{R} \setminus \{0\}$, we obtain

$$\frac{\|F'(x)(th^*) - \hat{L}(th^*)\|}{\|th^*\|} = \frac{\|F'(x)h^* - \hat{L}h^*\|}{\|h^*\|} = \frac{a}{\|h^*\|},$$

which will not tend to 0 as $t \rightarrow 0$, contradicting (3.2). □

One can reformulate Definition 3.1.1 in terms of Landau notation: F is differentiable at $x \in X$ if there exists a bounded linear operator L such that

$$F(x+h) = F(x) + Lh + \Psi(h),$$

Chapter 3. Adjoint based analysis for nonlinear problems

with $\Psi(h) = o(h)$. In this setting an operator Ψ is little- o of h (written $\Psi(h) = o(h)$) if

$$\lim_{h \rightarrow 0} \frac{\|\Psi(h)\|_Y}{\|h\|_X} = 0.$$

It will be convenient to prove some properties of the little- o notation summarized in the following lemma:

Lemma 3.1.1. *Suppose $\Psi, \Phi : X \rightarrow Y$, $h \in X$, and $\alpha \in \mathbb{R}$. We have the following properties if $\Psi(h) = o(h)$ and $\Phi(h) = o(h)$:*

1. $\Psi(\alpha h) = o(h)$
2. $\Psi(h) + \Phi(h) = o(h)$
3. $\Psi(\Phi(h)) = o(h)$

Proof. By the definition of a limit, $\Psi(h) = o(h)$ if, given any $\varepsilon > 0$, we can find $\delta > 0$ such that

$$\frac{\|\Psi(h)\|}{\|h\|} \leq \varepsilon \implies \|\Psi(h)\| \leq \varepsilon \|h\|$$

provided $\|h\| \leq \delta$.

1. Take $g := \alpha h$. We assume $\Psi(h) = o(h)$ so given any $\tilde{\varepsilon} > 0$ can find a $\tilde{\delta} > 0$ such that

$$\|\Psi(\alpha h)\| = \|\Psi(g)\| \leq \tilde{\varepsilon} \|g\| = \tilde{\varepsilon} |\alpha| \|h\| = \varepsilon \|h\|,$$

whenever $\|g\| = |\alpha| \|h\| < \tilde{\delta}_1 \implies \|h\| \leq \delta$.

2. Given $\tilde{\varepsilon} > 0$, we can find $\delta_\Psi, \delta_\Phi > 0$

$$\|h\| < \delta_\Psi \implies \|\Psi(h)\| < \tilde{\varepsilon} \text{ and } \|h\| < \delta_\Phi \implies \|\Phi(h)\| < \tilde{\varepsilon}.$$

Therefore taking $\delta = \min\{\delta_\Psi, \delta_\Phi\}$, $\|h\| \leq \delta$ implies

$$\|\Psi(h) + \Phi(h)\| \leq \|\Psi(h)\| + \|\Phi(h)\| \leq \tilde{\varepsilon} \|h\| + \tilde{\varepsilon} \|h\| = \varepsilon \|h\|,$$

for $\varepsilon = 2\tilde{\varepsilon}$.

Chapter 3. Adjoint based analysis for nonlinear problems

3. Similarly as for 2, we can find $\delta_\Psi, \delta_\Phi > 0$

$$\|h\| < \delta_\Psi \implies \|\Psi(h)\| < \tilde{\varepsilon} \text{ and } \|h\| < \delta_\Phi \implies \|\Phi(h)\| < \tilde{\varepsilon}.$$

Again take $\delta = \min\{\delta_\Psi, \delta_\Phi\}$, and let $g := \Phi(h)$. Then $\|h\| \leq \delta$ implies

$$\|\Psi(\Phi(h))\| = \|\Psi(g)\| \leq \tilde{\varepsilon}\|g\| = \tilde{\varepsilon}\|\Phi(h)\| \leq \tilde{\varepsilon}^2\|h\| = \varepsilon\|h\|,$$

for $\varepsilon = \tilde{\varepsilon}^2$.

□

The Fréchet derivative enjoys many of the same properties as the derivative in \mathbb{R}^d , e.g. product rule, derivatives of trigonometric functions, etc. The proofs are the same as for \mathbb{R}^d since the limit definition is the same. We also have a version of the chain rule for the Fréchet derivative, which we prove here explicitly.

Theorem 3.1.1 (The chain rule). *Suppose X, Y, Z are Banach spaces with maps $F : U \rightarrow Y$ and $G : V \rightarrow Z$ where $U \subset X$ and $V = F(U)$ are open. Also suppose that F is differentiable on U and g is differentiable on V . Then for the composite map $F \circ G : U \rightarrow Z$, we have, for fixed $x_0 \in U$,*

$$(F \circ G)'(x_0)h = F'(y_0)G'(x_0)h, \tag{3.3}$$

where $y_0 = G(x_0)$.

Proof. We can find a ball $B_1 \subset U$ such that

$$G(x+h) = G(x) + G'(x)h + o(h) = y + G'(x)h + o(h),$$

for all $x \in B_1$. Let $k := G'(x)h + o(h)$. Then similarly, we can find another ball C_1 such that

$$F(y+k) = F(y) + F'(y)k + o(k).$$

Chapter 3. Adjoint based analysis for nonlinear problems

Now expanding the composite function about x ,

$$\begin{aligned} F(G(x+h)) &= F(y+k) = F(y) + F'(y)k + o(k) \\ &= F(y) + F'(y)G'(x)h + G'(x)o(h) + o(k) \\ &= F(y) + F'(y)G'(x)h + \Psi(h), \end{aligned}$$

where $\Psi(h) = G'(x)o(h) + o(k)$. Using the properties of Lemma 3.1.1 we conclude $\Psi(h) = o(h)$ and the result follows. \square

We now consider a version of the mean value theorem for integrals in this setting. First, consider F as before. We further specify the domain of F to be convex. Now define $\gamma(s)$ implicitly by $F \circ \gamma : [0, 1] \rightarrow Y$, $F \circ \gamma(s) = F(su + (1-s)v)$. This is well defined since, by convexity, the “line segment” $\{su + (1-s)v : s \in [0, 1]\}$ is contained in the domain of f . By the just established chain rule,

$$\frac{d}{ds}(F \circ \gamma(s)) = F'(su + (1-s)v)(u-v),$$

since the Fréchet derivative on \mathbb{R} is just the regular derivative. Integrating both sides with respect to s and applying the fundamental theorem of calculus on the LHS,

$$\begin{aligned} (F \circ \gamma(s))\Big|_0^1 &= \int_0^1 F'(su + (1-s)v)(u-v) ds \\ \implies F(u) - F(v) &= \left(\int_0^1 F'(su + (1-s)v) ds \right) (u-v). \end{aligned} \quad (3.4)$$

We have just proven the following

Theorem 3.1.2. *For any $u, u_h \in X$, If we choose*

$$\bar{F} = \int_0^1 F'(su + (1-s)u_h) ds,$$

then we have the following property

$$\bar{F}(u - u_h) = F(u) - F(u_h).$$

Remark 3.1.1. We remark that in practice we do not have access to the true solution u , and so we must linearize by replacing the true solution with the computed solution,

$$\bar{F} = \int_0^1 F'(u_h + s(u_h - u_h)) ds = F'(u_h).$$

Again in analogy with \mathbb{R}^d there is a weaker notion of derivative, namely the Gâteaux derivative.

Definition 3.1.2. Let $F : X \rightarrow Y$. We define the Gâteaux derivative in the direction $h \in X$, $\mathcal{G}_h[f] : X \rightarrow Y$ by

$$\mathcal{G}_h[F](u) = \lim_{t \rightarrow 0} \frac{F(u + th) - F(u)}{t}.$$

We can compute Gâteaux derivative by introducing, for a fixed $u, h \in X$, the function of a real variable $\tilde{F}(\varepsilon) = F(u + \varepsilon h)$, then

$$\left. \frac{d\tilde{F}}{d\varepsilon} \right|_{\varepsilon=0} = \lim_{t \rightarrow 0} \left. \frac{F(u + (\varepsilon + t)h) - F(u + \varepsilon h)}{t} \right|_{\varepsilon=0} = \mathcal{G}_h[f](u). \quad (3.5)$$

We call the function \tilde{F} the *Gâteaux function* corresponding to $\mathcal{G}_h[F]$. Note that the Gâteaux derivative, and hence the corresponding Gâteaux function, is not in general linear or continuous in h . However, if the Fréchet derivative exists, we do have both of these properties.

Theorem 3.1.3. Suppose F is (Fréchet) differentiable at $a \in U$. Then $\mathcal{G}_h[F]$ is continuous and linear in h , and in particular,

$$\mathcal{G}_h[F](u) = F'(u)h$$

for any $h \in X$.

Proof. This follows immediately from (3.5) and the chain rule,

$$\mathcal{G}_h[F](u) = \left. \frac{d\tilde{F}}{d\varepsilon} \right|_{\varepsilon=0} = \left. \frac{d}{d\varepsilon} F(u + \varepsilon h) \right|_{\varepsilon=0} = F'(u + \varepsilon h)h \Big|_{\varepsilon=0} = F'(u)h.$$

□

Chapter 3. Adjoint based analysis for nonlinear problems

We now return to the question of the what choice of linearization to take to satisfy the heuristic in (3.1). In this case the linear operator \bar{F} is actually a function of the error $\bar{F} = A(e)$ so we *define* the adjoint to F by the adjoint in the linear sense to $A(e)$, denoted $A^*(e)$. Returning to the problem at hand, recall our nonlinear operator is given by $F(u) = \nabla^2 u + \mathbf{b} \cdot \nabla u + u^2$. Consider real function

$$\begin{aligned}\tilde{F}(\varepsilon) &= F(u + \varepsilon h) = \nabla^2(u + \varepsilon h) + \mathbf{b} \cdot \nabla(u + \varepsilon h) + (u + \varepsilon h)^2 \\ &= \nabla^2 u + \varepsilon \nabla^2 h + \mathbf{b} \cdot (\nabla u + \varepsilon \nabla h) + u^2 + 2\varepsilon u h + (\varepsilon h)^2\end{aligned}$$

We compute the Gâteaux derivative by way of the Gâteaux function:

$$\begin{aligned}\left. \frac{d\tilde{F}}{d\varepsilon} \right|_{\varepsilon=0} &= \nabla^2 h + \mathbf{b} \cdot \nabla h + 2uh + 2\varepsilon h \Big|_{\varepsilon=0} \\ &= \nabla^2 h + \mathbf{b} \cdot \nabla h + 2uh = F'(u)h,\end{aligned}$$

by Theorem 3.1.3. Thus,

$$\begin{aligned}\bar{F}v &= A(e)v = \int_0^1 F'(su + (1-s)u_h)v \, ds \\ &= \int_0^1 \nabla^2 v + \mathbf{b} \cdot \nabla v + 2(su + (1-s)u_h)v \, ds \\ &= \nabla^2 v + \mathbf{b} \cdot \nabla v + (u + u_h)v.\end{aligned}$$

Note if we substitute $v = e$,

$$\begin{aligned}A(e)e &= \nabla^2 e + \mathbf{b} \cdot \nabla e + (u + u_h)e \\ &= \nabla^2(u - u_h) - \mathbf{b} \cdot \nabla(u - u_h) + u^2 - u_h^2 \\ &= F(u) - F(u_h),\end{aligned}$$

which agrees with our heuristic (3.1). The adjoint operator is then

$$A^*(e)w = \nabla^2 w - \mathbf{b} \cdot \nabla w + (u + u_h)w.$$

We conclude this section by proving some additional properties of the Fréchet derivative that will aide us in future computation. We note that in the example presented, the linear terms in our operator were fixed under the action of the derivative. This is not a coincidence, as demonstrated in the following proposition

Proposition 3.1.2. *If $F : X \rightarrow Y$ is linear then for any $u, h \in X$,*

$$Fh = F'(u)h.$$

Proof. The argument is the same as for the derivative in \mathbb{R}^d . From the definition of the Fréchet derivative

$$\lim_{h \rightarrow 0} \frac{\|F(u+h) - Fu - Lh\|_Y}{\|h\|_X} = \lim_{h \rightarrow 0} \frac{\|Fh - Lh\|_Y}{\|h\|_X}.$$

Thus, the numerator is identically 0 if $F = L = F'$. By uniqueness of the Fréchet derivative, we are done. \square

There is also an easy formula for Fréchet derivatives involving functions of real derivatives.

Proposition 3.1.3. *Let $x(t) \in X$ and consider the derivative $F(x) = \frac{dx}{dt}$. Then we have that*

$$F'(x)h = \frac{dh}{dt}. \quad (3.6)$$

Proof. From Definition 3.1.1

$$\frac{\|\frac{d}{dt}(x+h) - \frac{dx}{dt} - Lh\|_Y}{\|h\|_X} = \frac{\|\frac{dh}{dt} - Lh\|_Y}{\|h\|_X}. \quad (3.7)$$

Clearly if we choose $L = \frac{d}{dt}$ the numerator is 0 for all h , so by uniqueness of the Fréchet derivative, we are done. \square

We now present a version of the product rule for the Fréchet derivative. This is achieved through by combining the following Lemmas

Lemma 3.1.2. *Let X, Y, Z be Banach spaces and define the continuous bilinear form, $B : X \times Y \rightarrow Z$ Then B is Fréchet differentiable at $(x_0, y_0) \in X \times Y$ and it's Fréchet derivative is the linear map $B'(x_0, y_0) : X \times Y \rightarrow Z$ given by*

$$B'(x_0, y_0)(x, y) = B(x_0, y) + B(x, y_0). \quad (3.8)$$

Chapter 3. Adjoint based analysis for nonlinear problems

Proof. We take advantage of (3.5) and Theorem 3.1.3,

$$B'(x_0, y_0)(x, y) = \left. \frac{d\tilde{B}}{d\varepsilon} \right|_{\varepsilon=0}$$

where $\tilde{B}(\varepsilon) = B(x_0 + \varepsilon x, y_0 + \varepsilon y)$. Computing,

$$\begin{aligned} \left. \frac{d\tilde{B}}{d\varepsilon} \right|_{\varepsilon=0} &= \left. \frac{d}{d\varepsilon} [B(x_0 + \varepsilon x, y_0 + \varepsilon y)] \right|_{\varepsilon=0} \\ &= \left. \frac{d}{d\varepsilon} [B(x_0 + \varepsilon x, y_0) + B(x_0 + \varepsilon x, \varepsilon y)] \right|_{\varepsilon=0} \\ &= \left. \frac{d}{d\varepsilon} [B(x_0, y_0) + B(\varepsilon x, y_0) + B(x_0, \varepsilon y) + B(\varepsilon x, \varepsilon y)] \right|_{\varepsilon=0} \\ &= \left. \frac{d}{d\varepsilon} [B(x_0, y_0) + \varepsilon B(x, y_0) + \varepsilon B(x_0, y) + \varepsilon^2 B(x, y)] \right|_{\varepsilon=0} \\ &= B(x, y_0) + B(x_0, y) + 2\varepsilon B(x, y) \Big|_{\varepsilon=0} \\ &= B(x, y_0) + B(x_0, y). \end{aligned}$$

□

Finally, we have the differentiation rule for parameterized functions,

Lemma 3.1.3. *Let X, Y be a Banach spaces with $F, G : X \rightarrow Y$. Then if $H : X \rightarrow Y \times Y, H(x) = (F(x), G(x))$ is Fréchet differentiable, the derivative is given by*

$$H'(x) = (F'(x), G'(x)). \quad (3.9)$$

Proof. Proceeding in the same way as the proof of the previous lemma, now with $\tilde{H}(\varepsilon) = H(x_0 + \varepsilon x)$,

$$\left. \frac{d\tilde{H}}{d\varepsilon} \right|_{\varepsilon=0} = \left. \frac{d}{d\varepsilon} (F(x_0 + \varepsilon x), G(x_0 + \varepsilon x)) \right|_{\varepsilon=0} = \left(\left. \frac{d\tilde{F}}{d\varepsilon}, \frac{d\tilde{G}}{d\varepsilon} \right) \right|_{\varepsilon=0} = (F'(x), G'(x)).$$

□

Next we combine the previous lemmas along with the chain rule,

Theorem 3.1.4 (Product rule in Banach spaces). *Let X, Y, Z, W be Banach spaces and $F : X \rightarrow Y, G : X \rightarrow Z$, are Fréchet differentiable maps. Also define the product form, $B : Y \times Z \rightarrow W$. Then the product function $\Psi : X \rightarrow W$ given by $\Psi(x) = B(F(x), G(x))$ is Fréchet differentiable at $x \in X$ and it's derivative for a fixed $x_0 \in X$ is the linear map $\Psi'(x_0) : X \rightarrow W$ given by*

$$\Psi'(x_0)x = B(F(x_0), G'(x_0))x + B(G(x_0), F'(x_0))x. \quad (3.10)$$

Proof. We realize Ψ is a composite function, $\Psi(x) = F(x)G(x) = (B \circ H)(x)$. Thus, using the previous lemmas, and the chain rule,

$$\begin{aligned} \Psi'(x) &\stackrel{(3.3)}{=} B'(F(x), G(x))H'(x) \stackrel{(3.9)}{=} B'(F(x), G(x))(F'(x), G'(x)) \\ &\stackrel{(3.8)}{=} B(F(x), G'(x)) + B(F'(x), G(x)). \end{aligned}$$

□

We will make use of the following corollaries throughout the rest of this thesis

Corollary 1. Set $X = \mathbf{H}^1(\Omega), Y = X^d, Z = W = X$ and $B(x, A) = Ax$ is matrix-vector multiplication on $X \times Y$. Then if we take $F(\mathbf{u}) = \nabla \mathbf{u}, G(\mathbf{u}) = \mathbf{u}$,

$$\frac{\partial}{\partial \mathbf{u}} [(\nabla \mathbf{u})\mathbf{u}]\mathbf{v} = (\nabla \mathbf{u})\mathbf{v} + (\nabla \mathbf{v})\mathbf{u}, \quad (3.11)$$

Corollary 2. If we take $X = Y = Z = W = \mathbf{H}^1(\Omega)$ and $B(\mathbf{u}, \mathbf{v}) = \mathbf{u} \times \mathbf{v}$ and $F(\mathbf{u}) = \nabla \times \mathbf{u}, G(\mathbf{u}) = \mathbf{u}$,

$$\frac{\partial}{\partial \mathbf{u}} [(\nabla \times \mathbf{u}) \times \mathbf{u}]\mathbf{v} = (\nabla \times \mathbf{u}) \times \mathbf{v} + (\nabla \times \mathbf{v}) \times \mathbf{u}. \quad (3.12)$$

Note that these corollaries are also implicitly appealing to Proposition 3.1.3.

3.2 Adjoint based analysis for the nonlinear viscous Burgers equation

In this section, we consider the case of a quasilinear PDE, namely the steady state viscous Burgers equation. In one dimension with $\Omega = (0, 1)$, the problem is

$$-\nu u'' + uu' = f, \quad \text{in } \Omega \quad (3.13a)$$

$$u = 0, \quad \text{on } \partial\Omega, \quad (3.13b)$$

where $f(x) = \pi^2 \sin(\pi x) + \pi \sin(\pi x) \cos(\pi x)$ is chosen to manufacture $u(x) = \sin(\pi x)$. We use the QoI $\mathcal{Q}(u) = (u, \psi)$ where $\psi \equiv 1$, i.e. the average value of the solution in our unit domain. In order to perform an adjoint analysis, we must again linearize about the error as outlined in the previous sections. Define the nonlinear operator F by

$$F(w) = -\nu w'' + ww' \quad (3.14)$$

so that $F(u(x)) = f(x)$. We compute the Fréchet derivative using the standard product and chain rule as well as Proposition 3.1.3 to compute

$$F'(w)h = -\nu h'' + wh' + w'h. \quad (3.15)$$

In accord with Theorem 3.1.2 we define our linearized operator \bar{F} with error $e = u - u_h$ for a computed solution u_h by

$$\begin{aligned} \bar{F}h &= \int_0^1 F'(su + (1-s)u_h)h \, ds \\ &= \int_0^1 -\nu h'' + (su + (1-s)u_h)h' + (su + (1-s)u_h)'h \, ds \\ &= -\nu h'' + u_h h' + u_h' h + \int_0^1 s(u - u_h)h' + s(u - u_h)'h \, ds \\ &= -\nu h'' + u_h h' + u_h' h + \frac{1}{2}(u - u_h)h' + \frac{1}{2}(u - u_h)'h \\ &= -\nu h'' + \frac{1}{2}u_h h' + \frac{1}{2}u_h' h + \frac{1}{2}u h' + \frac{1}{2}u' h. \end{aligned}$$

Chapter 3. Adjoint based analysis for nonlinear problems

To check this is the correct definition, we simply plug in $e = (u - u_h)$ for h ,

$$\begin{aligned}
 \bar{F}(u - u_h) &= -\nu(u'' - u_h'') + u_h(u' - u_h') + u_h'(u - u_h) + (u - u_h)(u' - u_h') \\
 &= [-\nu u + uu'] + \nu u_h'' + u_h u' - u_h u_h' + u_h' u - u_h' u_h - u u_h' - u_h u' + u_h u_h' \\
 &= F(u) - [-\nu u_h'' + u_h u_h'] = F(u) - F(u_h).
 \end{aligned} \tag{3.16}$$

We should emphasize here that we are considering u, u_h fixed so that \bar{F} is indeed linear in its argument.

We now seek an adjoint to \bar{F} in the standard way. The primal weak problem is find: $u \in H_0^1(\Omega)$ such that

$$\begin{aligned}
 (\bar{F}w, v) &= (-\nu w'', v) + \left(\frac{1}{2}u_h w' + \frac{1}{2}u w', v\right) + \left(\frac{1}{2}u_h' w + \frac{1}{2}u' w, v\right) \\
 &= (\nu w', v') + \left(w', \frac{1}{2}u_h v + \frac{1}{2}u v\right) + \left(w, \frac{1}{2}(u_h' v + u' v)\right) \\
 &= (\nu w', v') - \left(w, \frac{1}{2}(u_h' v + v' u_h + u' v + v' u)\right) + \left(w, \frac{1}{2}(u_h' v + u' v)\right) \\
 &= (\nu w, v'') - \left(w, \frac{1}{2}(v' u_h + v' u)\right) \\
 &= (w, \bar{F}^* v).
 \end{aligned}$$

We conclude the strong form adjoint problem to the linearized operator \bar{F} is

$$-\nu \phi'' - \frac{1}{2}(\phi' u_h + \phi' u) = \psi, \quad x \in \Omega, \tag{3.17a}$$

$$\phi = 0, \quad x \in \partial\Omega. \tag{3.17b}$$

The corresponding weak adjoint problem is find $\phi \in H_0^1(\Omega)$ such that

$$a^*(\phi, v) := (\nu \phi', v') - \left(\frac{1}{2}(\phi' u_h + \phi' u), v\right) = (\psi, v), \quad \forall v \in H_0^1(\Omega). \tag{3.18}$$

This leads us to the following theorem

Theorem 3.2.1. *Given a quantity of interest $\mathcal{Q}(u) = (\psi, u)$, we have the following error representation*

$$(\psi, e) = (\phi, f) - (\phi, F(u_h)),$$

where ϕ solves the dual problem (3.18).

Proof. The proof follows the properties of the adjoint and our choice of linearization,

$$(\psi, e) = a^*(\phi, e) = (\bar{F}^* \phi, e) \stackrel{(3.16)}{=} (\phi, F(u) - F(u_h)) = (\phi, f) - (\phi, F(u_h)). \quad (3.19)$$

□

In practice, we must numerically approximate the solution ϕ_h to (3.18) and we also incur linearization error as described in Remark 3.1.1. This leads to defining the error estimate, η_{burg} for a given approximate generalized Green's function ϕ_h ,

$$\eta_{burg} = (\phi_h, f) - (\phi_h, F(u_h)) \approx (\psi, e). \quad (3.20)$$

Note that in general we use a higher order/finer discretization to approximate ϕ_h than we do for u_h . In a finite element context, this is to avoid the estimate η_{burg} being zero due to Galerkin orthogonality.

3.2.1 Numerical experiment for Burgers equation

In this experiment we discretize the domain Ω using the finite element method. In particular, we use a uniform triangulation \mathcal{T}_h (partition in 1D) of Ω and the standard continuous Galerkin Lagrange space discussed in Appendix A, and in particular we use the space \mathbb{P}^1 for u . We then define the effectivity ratio, denoted Eff., characterizes how well the error estimate approximates the true error, given an estimator η ,

$$\text{Eff.} = \frac{\text{Error estimate}}{\text{True error}} = \frac{\eta}{(\psi, e)}. \quad (3.21)$$

The closer the effectivity is to 1, the better the error estimate provided by our method. For an increasing refinement of the mesh, we show effectivities in Table 3.1. The effectivities are very close to 1, indicating that the solution of the adjoint problem is quite accurate, despite the linearization error and numerical approximation ϕ_h of ϕ .

Number of Elements	True Error in QoI	Eff.
128	3.16e-05	1.00
256	7.90e-6	1.00
512	1.97e-6	1.00
1024	4.93e-7	1.00

Table 3.1: Effectivity ratios (3.21) for the problem outlined in §3.2 using the error estimate (3.20). The true QoI is exactly $\frac{2}{\pi}$ in this case.

3.3 Adjoint analysis for nonlinearity and Neumann boundary conditions

Let $\Omega = (0, 1)^2 \subset \mathbb{R}^2$. In this section we seek a error estimate for the QoI $\mathcal{Q}(u) = \frac{1}{4}(u, \psi)$ where

$$\psi(x) = \begin{cases} 1, & x \in \Omega_c = [\frac{1}{4}, \frac{3}{4}] \times [0, \frac{1}{2}], \\ 0, & \text{otherwise.} \end{cases}$$

In other words, the QoI is the average value of the solution in Ω_c . The true solution u solves

$$\begin{aligned} -\nabla^2 u + \mathbf{b} \cdot \nabla u + \sin(u) &= s(x, y), \quad \text{in } \Omega, \\ u &= 0, \quad \text{on } \Gamma_D := \{x = 0 \text{ or } x = 1\}, \\ \frac{\partial u}{\partial n} &= 0, \quad \text{on } \Gamma_N := \{y = 0 \text{ or } y = 1\}, \end{aligned} \tag{3.22}$$

where

$$\begin{aligned} s(x, y) &= 2b_y \pi \cos(2\pi x) \cos(2\pi y) - 2b_x \pi \sin(2\pi x) \sin(2\pi y) \\ &\quad + 8\pi^2 (\cos(2\pi x) \sin(2\pi y)) + \sin(\cos(\pi x) \sin(2\pi y)) \end{aligned} \tag{3.23}$$

is chosen to manufacture $u(x, y) = \cos(2\pi x) \sin(2\pi y)$. We take a constant convection field $\mathbf{b} = [b_x, b_y]^T = [4, 4]^T$. We first apply the linearization process of the last section since there is nonlinearity present, namely $\sin(u)$. The nonlinear operator associated with the problem (3.22) is

$$F(v) = -\nabla^2 v + \mathbf{b} \cdot \nabla v + \sin(v)$$

Chapter 3. Adjoint based analysis for nonlinear problems

We compute the Fréchet derivative by way of (3.5). Let $g(\varepsilon) = F(u + \varepsilon h)$. Then we compute

$$F'(u)h = \left. \frac{dg}{d\varepsilon} \right|_{\varepsilon=0} = -\nabla^2 h + \mathbf{b} \cdot \nabla h + \left. \frac{d}{d\varepsilon} \sin(u + \varepsilon h) \right|_{\varepsilon=0} = -\nabla^2 h + \mathbf{b} \cdot \nabla h + \cos(u)h, \quad (3.24)$$

Again, appealing to Theorem 3.1.2 the linearized operator is

$$\begin{aligned} \bar{F}v &= \int_0^1 F'(su + (1-s)u_h)v \, ds \\ &= -\nabla^2 v + \mathbf{b} \cdot \nabla v + \int_0^1 \cos(su + (1-s)u_h) \, ds \, v \\ &= -\nabla^2 v + \mathbf{b} \cdot \nabla v + Iv, \end{aligned}$$

where $Iv = \int_0^1 \cos(su + (1-s)u_h) \, ds \, v$. We now compute the adjoint to this linearized operator \bar{F} based on the strong definition of the adjoint described in §2.1. Let $H_0^1(\Omega) := \{v \in H^1 : v = 0 \text{ on } \Gamma_D\}$ be our space of test functions. Multiplying $\bar{F}u$ by $v \in H_0^1(\Omega)$ and integrating over Ω ,

$$\begin{aligned} (-\nabla^2 u, v) + (\mathbf{b} \cdot \nabla u, v) + (Iu, v) &\stackrel{\text{(B.7)}}{=} (\nabla u, \nabla v) + (v, \nabla u \cdot \mathbf{n})_\Gamma + (\mathbf{b} \cdot \nabla u, v) + (Iu, v) \\ &= (\nabla u, \nabla v) + (\mathbf{b} \cdot \nabla u, v) + (Iu, v), \end{aligned}$$

since $v = 0$ on Γ_D and $\nabla u \cdot \mathbf{n} = 0$ on Γ_N . This leads us to the definition of the primal bilinear form associated to \bar{F} :

$$a(u, v) := (\nabla u, \nabla v) + (\mathbf{b} \cdot \nabla u, v) + (Iu, v). \quad (3.25)$$

To obtain an adjoint problem, we also perform integration by parts on the convection term,

$$(\mathbf{b} \cdot \nabla u, v) = (u, -\nabla \cdot (v\mathbf{b})) + (u, \mathbf{n} \cdot (v\mathbf{b}))_\Gamma = -(u, \mathbf{b} \cdot \nabla v) + (u, v(\mathbf{n} \cdot \mathbf{b}))_{\Gamma_N}, \quad (3.26)$$

as well as another integration by parts again on the diffusion term,

$$(\nabla u, \nabla v) = -(u, \nabla^2 v) + (u, \mathbf{n} \cdot \nabla v)_\Gamma. \quad (3.27)$$

The linearized term is trivial since it is just a constant,

$$(\bar{I}u, v) = (u, \bar{I}v). \quad (3.28)$$

We conclude the strong linearized adjoint problem corresponding (3.22) is

$$\begin{aligned} -\nabla^2\phi - \mathbf{b} \cdot \nabla\phi + \bar{I}\phi &= \psi(x, y), & \text{in } \Omega, \\ \phi &= 0, & \text{on } \Gamma_D \\ \frac{\partial\phi}{\partial\mathbf{n}} + (\mathbf{n} \cdot \mathbf{b})\phi &= 0, & \text{on } \Gamma_N. \end{aligned} \quad (3.29)$$

and the corresponding weak adjoint problem is: find $\phi \in H_0^1(\Omega)$ such that

$$a^*(\phi, v) := (\nabla\phi, \nabla v) - (v, \mathbf{b} \cdot \nabla\phi) + (v, \phi(\mathbf{n} \cdot \mathbf{b}))_{\Gamma_N} + (v, I\phi) = (\psi, v), \quad (3.30)$$

for all $v \in H_0^1(\Omega)$. We have the following error representation, for ϕ exactly solving 3.30,

$$\begin{aligned} (e, \psi) &= a^*(\phi, e) = a(e, \phi) = (\nabla e, \nabla\phi) + (\mathbf{b} \cdot \nabla e, \phi) + (\bar{I}e, \phi) \\ &= (\nabla u, \nabla\phi) + (\mathbf{b} \cdot \nabla u, \phi) + (\cos(u), \phi) - ((\nabla u_h, \nabla\phi) + (\mathbf{b} \cdot \nabla u_h, \phi) + (\cos(u_h), \phi)) \\ &= (s, \phi) - (\nabla u_h, \nabla\phi) - (\mathbf{b} \cdot \nabla u_h, \phi) - (\cos(u_h), \phi). \end{aligned}$$

Due to the linearization error mentioned in Remark 3.1.1 as well as the fact that we must solve the adjoint problem (3.30) numerically, we introduce the error estimator η_{rob} given by

$$\eta_{rob} = (s, \phi_h) - (\nabla u_h, \nabla\phi_h) - (\mathbf{b} \cdot \nabla u_h, \phi_h) - (\cos(u_h), \phi_h), \quad (3.31)$$

for a computed Green's function ϕ_h .

3.3.1 Numerical experiment for Neumann BCs

We use a uniform simplicial discretization \mathcal{T}_h for Ω , see Figure 3.1 for an example mesh. We use Galerkin Langrange space described in Appendix A for the scalar

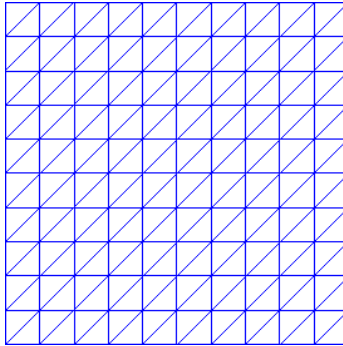


Figure 3.1: A sample 10×10 triangulation for the unit square, \mathcal{T}_h .

Number of Elements	True Error in QoI	Eff.
16^2	4.87e-3	0.97
32^2	1.23-3	0.99
64^2	3.04-4	1.00
128^2	7.58e-5	1.00

Table 3.2: Effectivity ratios (3.21) for the problem outlined in §3.3 using the error estimate (3.31).

unknown, in this case \mathbb{P}^1 for u . Results are given in Table 3.2. Again note that the effectivity (3.21) (although now using η_{rob} for the estimator) is very close to 1, so estimator is accurate despite the approximation of the computed solution for the true solution in the definition of the adjoint.

3.3.2 Vanishing boundary conditions

In the previous section, we defined our space of test functions, $H_0^1(\Omega)$, to only vanish on the Dirichlet boundary, Γ_D . However, we can equally well define $H_0^1(\Omega) := \{v \in H^1(\Omega) : v = 0 \text{ on } \partial\Omega = \Gamma_D \cup \Gamma_N\}$. If we do this, note that the $(u, v(\mathbf{n} \cdot \mathbf{b}))_{\Gamma_N}$ term vanishes in (3.26).

3.4 Adjoint based analysis for the incompressible Navier-Stokes equations

We now consider a problem with a “natural” nonlinearity: the incompressible stationary Navier-Stokes equations. The equations are given by

$$-\nu\Delta\mathbf{u} + \mathcal{C}(\mathbf{u}) + \nabla p = \mathbf{f}, \quad \text{in } \Omega, \quad (3.32a)$$

$$\nabla \cdot \mathbf{u} = 0, \quad \text{in } \Omega, \quad (3.32b)$$

$$\mathbf{u} = \mathbf{0}, \quad \text{on } \Gamma_D, \quad (3.32c)$$

$$-p\mathbf{n} + \nu(\mathbf{n} \cdot \nabla)\mathbf{u} = \mathbf{0}, \quad \text{on } \Gamma_N. \quad (3.32d)$$

where

$$\mathcal{C}(\mathbf{u}) := (\mathbf{u} \cdot \nabla)\mathbf{u} = \sum_{i=1}^d u_i \partial_{x_i} \mathbf{u} = (\nabla \mathbf{u})\mathbf{u} \quad (3.33)$$

and the last equality follows because in general

$$(\nabla \mathbf{v})\mathbf{u} = \begin{bmatrix} \mathbf{u}^T \nabla v_1 \\ \vdots \\ \mathbf{u}^T \nabla v_d \end{bmatrix} = \sum_{i=1}^d u_i \partial_{x_i} \mathbf{v}. \quad (3.34)$$

The unknowns are the velocity \mathbf{u} and pressure p . The viscosity ν and forcing function \mathbf{f} are considered as data to the problem. We must proceed as in the previous section by first linearizing about the error. However, by Proposition 3.1.2 and linearity of the Fréchet derivative, it suffices to compute the derivative of only the nonlinear terms. The only nonlinear term is $\mathcal{C}(\mathbf{u})$ which we already know the derivative for from Corollary 1,

$$\frac{\partial \mathcal{C}}{\partial \mathbf{u}} \mathbf{v} = \frac{\partial}{\partial \mathbf{u}} [(\nabla \mathbf{u})\mathbf{u}] \mathbf{v} \stackrel{(3.11)}{=} (\nabla \mathbf{u})\mathbf{v} + (\nabla \mathbf{v})\mathbf{u} = (\mathbf{u} \cdot \nabla)\mathbf{v} + (\mathbf{v} \cdot \nabla)\mathbf{u}.$$

we define the linearized operator by

$$\begin{aligned}
\bar{\mathcal{C}}\mathbf{w} &= \int_0^1 \frac{\partial \mathcal{C}}{\partial \mathbf{u}}(s\mathbf{u} + (1-s)\mathbf{u}_h)\mathbf{w} \, ds \\
&= \int_0^1 ((s\mathbf{u} + (1-s)\mathbf{u}_h) \cdot \nabla)\mathbf{w} + (\mathbf{w} \cdot \nabla)(s\mathbf{u} + (1-s)\mathbf{u}_h) \, ds \\
&= (\mathbf{u}_h \cdot \nabla)\mathbf{w} + (\mathbf{w} \cdot \nabla)\mathbf{u}_h + \int_0^1 s [((\mathbf{u} - \mathbf{u}_h) \cdot \nabla)\mathbf{w} + (\mathbf{w} \cdot \nabla)(\mathbf{u} - \mathbf{u}_h)] \, ds \\
&= (\mathbf{u}_h \cdot \nabla)\mathbf{w} + (\mathbf{w} \cdot \nabla)\mathbf{u}_h + \frac{1}{2} [((\mathbf{u} - \mathbf{u}_h) \cdot \nabla)\mathbf{w} + (\mathbf{w} \cdot \nabla)(\mathbf{u} - \mathbf{u}_h)] \\
&= \frac{1}{2} [(\mathbf{u} \cdot \nabla)\mathbf{w} + (\mathbf{w} \cdot \nabla)\mathbf{u} + (\mathbf{u}_h \cdot \nabla)\mathbf{w} + (\mathbf{w} \cdot \nabla)\mathbf{u}_h] \\
&= \frac{1}{2} [((\mathbf{u} + \mathbf{u}_h) \cdot \nabla)\mathbf{w} + (\mathbf{w} \cdot \nabla)(\mathbf{u} + \mathbf{u}_h)]
\end{aligned} \tag{3.35}$$

To find the adjoint operator, $\bar{\mathcal{C}}^*$, we must isolate \mathbf{w} . To this end, we multiply by a vector test function $\mathbf{v} \in \mathbf{H}_0^1(\Omega)$ and integrate over Ω . To simplify, we first set $\mathbf{s} := \mathbf{u} + \mathbf{u}_h$. Next we multiply (3.35) by $\mathbf{v} \in \mathbf{H}_0^1(\Omega)$,

$$\begin{aligned}
(\mathbf{v}, \bar{\mathcal{C}}\mathbf{w}) &= \frac{1}{2} [(\mathbf{v}, (\mathbf{s} \cdot \nabla)\mathbf{w}) + (\mathbf{v}, (\mathbf{w} \cdot \nabla)\mathbf{s})] \\
&= \frac{1}{2} \left[\int_{\Omega} \mathbf{v}^T (\nabla \mathbf{w}) \mathbf{s} \, dx + \int_{\Omega} \mathbf{v}^T (\nabla \mathbf{s}) \mathbf{w} \, dx \right] \\
&= \frac{1}{2} \left[\int_{\Omega} \mathbf{s}^T (\nabla \mathbf{w})^T \mathbf{v} \, dx + \int_{\Omega} \mathbf{w}^T (\nabla \mathbf{s})^T \mathbf{v} \, dx \right] \\
&= \frac{1}{2} [(\mathbf{s}, (\nabla \mathbf{w})^T \mathbf{v}) + (\mathbf{w}, (\nabla \mathbf{s})^T \mathbf{v})].
\end{aligned}$$

For the first term inside the brackets,

$$\begin{aligned}
(\mathbf{s}, (\nabla \mathbf{w})^T \mathbf{v}) &= \left(\mathbf{s}, \sum_{i=1}^d v_i \nabla w_i \right) \\
&= \int_{\Omega} \sum_{i=1}^d v_i \mathbf{s} \cdot \nabla w_i \, dx \\
&\stackrel{\text{(B.7)}}{=} - \int_{\Omega} \sum_{i=1}^d w_i \nabla \cdot (v_i \mathbf{s}) \, dx + \int_{\Gamma_N} \sum_{i=1}^d (w_i v_i) \mathbf{s} \cdot \mathbf{n} \, ds \\
&\stackrel{\text{(B.4)}}{=} - \int_{\Omega} \sum_{i=1}^d w_i (v_i \nabla \cdot \mathbf{s} + \nabla v_i \cdot \mathbf{s}) \, dx + \int_{\Gamma_N} \sum_{i=1}^d (w_i v_i) \mathbf{s} \cdot \mathbf{n} \, ds \\
&= \int_{\Omega} \mathbf{w} \cdot [-(\nabla \cdot \mathbf{s})\mathbf{v} - (\nabla \mathbf{v})\mathbf{s}] \, dx + \int_{\Gamma_N} \mathbf{w} \cdot (\mathbf{s} \cdot \mathbf{n})\mathbf{v} \, ds \\
&= (\mathbf{w}, -(\mathbf{s} \cdot \nabla)\mathbf{v} - (\nabla \cdot \mathbf{s})\mathbf{v}) + (\mathbf{w}, (\mathbf{n} \cdot \mathbf{s})\mathbf{v})_{\Gamma_N}
\end{aligned}$$

We conclude the linearized adjoint operator to $\bar{\mathcal{C}}$ should be

$$\bar{\mathcal{C}}^* \phi = \frac{1}{2} [(\nabla(\mathbf{u} + \mathbf{u}_h))^T \phi - ((\mathbf{u} + \mathbf{u}_h) \cdot \nabla) \phi - (\nabla \cdot (\mathbf{u} + \mathbf{u}_h)) \phi] \quad (3.36)$$

$$= \frac{1}{2} \left[\sum_{i=1}^d \phi_i \nabla(u_i + u_{ih}) - (u_i + u_{ih}) \partial_{x_i} \phi - (\nabla \cdot (\mathbf{u} + \mathbf{u}_h)) \phi \right] \quad (3.37)$$

with boundary contribution

$$\frac{1}{2} (\mathbf{n} \cdot (\mathbf{u} + \mathbf{u}_h)) \phi, \text{ on } \Gamma_N. \quad (3.38)$$

To find the adjoint operator corresponding to the linear terms, we first establish the primal weak form as an intermediate step. We multiply (3.32a) by $\mathbf{v} \in \mathcal{V} := \mathbf{H}_0^1(\Omega)$ and (3.32b) by $q \in \mathcal{Q} := [L^2(\Omega)]^d$ and integrate over Ω yielding

$$-(\nu \nabla^2 \mathbf{u}, \mathbf{v}) + (\mathcal{C}(\mathbf{u}), \mathbf{v}) + (\nabla p, \mathbf{v}) + (\nabla \cdot \mathbf{u}, q) = (\mathbf{f}, \mathbf{v}). \quad (3.39)$$

For the first term in (3.39),

$$\begin{aligned} & - \int_{\Omega} \nu \Delta \mathbf{u} \cdot \mathbf{v} \, dx = -\nu \int_{\Omega} \sum_{i=1}^d \Delta u_i v_i \, dx \\ & = \nu \int_{\Omega} \sum_{i=1}^d \nabla u_i \cdot \nabla v_i \, dx - \int_{\Gamma_N} \sum_{i=1}^d \nu (v_i \nabla u_i) \cdot \mathbf{n} \, ds \\ & = \int_{\Omega} \nu \nabla \mathbf{u} : \nabla \mathbf{v} \, dx - \int_{\Gamma_N} \mathbf{v} \cdot (\nu \mathbf{n} \cdot \nabla \mathbf{u}) \, ds. \end{aligned}$$

for the third term in (3.39),

$$\begin{aligned} \int_{\Omega} \nabla p \cdot \mathbf{v} \, dx & = - \int_{\Omega} p \nabla \cdot \mathbf{v} \, dx + \int_{\Gamma_N} p \mathbf{v} \cdot \mathbf{n} \, ds \\ & = - \int_{\Omega} p \nabla \cdot \mathbf{v} \, dx + \int_{\Gamma_N} \mathbf{v} \cdot (p \mathbf{n}) \, ds. \end{aligned}$$

From the boundary condition on Γ_N , the total contribution is 0. We can now pose our weak problem as

$$\mathcal{N}((\mathbf{u}, p), (\mathbf{v}, q)) = (\mathbf{f}, \mathbf{v}), \quad \forall (\mathbf{v}, q) \in \mathcal{V} \times \mathcal{Q}, \quad (3.40)$$

where the Navier Stokes form is defined as

$$\mathcal{N}_{NS}((\mathbf{u}, p), (\mathbf{v}, q)) := a(\mathbf{u}, \mathbf{v}) + c(\mathbf{u}, \mathbf{v}) - b(p, \mathbf{v}) + b(\mathbf{u}, q) \quad (3.41)$$

and in turn,

$$a(\mathbf{w}, \mathbf{v}) := \int_{\Omega} \nu \nabla \mathbf{w} : \nabla \mathbf{v} \, dx, \quad (3.42)$$

$$b(\mathbf{v}, q) := \int_{\Omega} q \nabla \cdot \mathbf{v} \, dx, \quad (3.43)$$

$$c(\mathbf{u}, \mathbf{v}) := \int_{\Omega} \mathcal{C}(\mathbf{u}) \mathbf{v} \, dx. \quad (3.44)$$

To find the adjoint operator, we must isolate the trial velocity \mathbf{u} ,

$$\begin{aligned} a(\mathbf{u}, \mathbf{v}) &= \int_{\Omega} \nu \nabla \mathbf{u} : \nabla \mathbf{v} \, dx = - \int_{\Omega} \mathbf{u} \cdot \nu \Delta \mathbf{v} \, dx + \int_{\Gamma_N} \mathbf{u} \cdot (\nu \mathbf{n} \cdot \nabla \mathbf{v}) \, ds, \\ b(\mathbf{u}, q) &= - \int_{\Omega} q \nabla \cdot \mathbf{u} \, dx = \int_{\Omega} \mathbf{u} \cdot \nabla q \, dx - \int_{\Gamma_N} \mathbf{u} \cdot (q \mathbf{n}) \, ds. \end{aligned}$$

Relabeling the test velocity \mathbf{v} with ϕ , and the test pressure q with π , we find the strong adjoint problem is

$$-\nu \nabla \phi + \bar{\mathcal{C}}^* \phi + \nabla \pi = \psi_{\mathbf{u}}, \quad \text{in } \Omega \quad (3.45a)$$

$$-\nabla \cdot \phi = \psi_p, \quad \text{in } \Omega \quad (3.45b)$$

$$\phi = \mathbf{0}, \quad \text{on } \Gamma_D \quad (3.45c)$$

$$\nu \mathbf{n} \cdot \nabla \phi - \pi \mathbf{n} + \frac{1}{2}((\mathbf{u} + \mathbf{u}_h) \cdot \mathbf{n}) \phi = \mathbf{0}, \quad \text{on } \Gamma_N. \quad (3.45d)$$

Upon multiplying by respective test functions $\mathbf{v} \in \mathcal{V}$ and $s \in \mathcal{Q}$ and integrating by parts, the corresponding weak adjoint problem is to find $(\phi, \pi) \in \mathcal{V} \times \mathcal{Q}$ such that

$$\mathcal{N}_{NS}^*((\phi, \pi), (\mathbf{v}, q)) = (\psi_{\mathbf{u}}, \mathbf{v}) + (\psi_p, q), \quad \forall (\mathbf{v}, q) \in \mathcal{V} \times \mathcal{Q}. \quad (3.46)$$

where the adjoint Navier-Stokes form is defined by

$$\mathcal{N}_{NS}^*((\phi, \pi), (\mathbf{v}, q)) := (\nu \nabla \phi, \nabla \mathbf{v}) + (\bar{\mathcal{C}}^* \phi, \mathbf{v}) - (\nabla \cdot \mathbf{v}, \pi) - (\nabla \cdot \phi, q). \quad (3.47)$$

If we denote $\mathbf{e}_{\mathbf{u}} := \mathbf{u} - \mathbf{u}_h$, $e_p := p - p_h$ and $\mathbf{e} = (\mathbf{e}_{\mathbf{u}}, e_p)^T$, we obtain the following representation for the error in a quantity of interest

Theorem 3.4.1. *Given a system QoI in the form of a linear functional represented by ψ , we have the following error representation*

$$(\psi, \mathbf{e}) = (\psi_{\mathbf{u}}, \mathbf{e}_{\mathbf{u}}) + (\psi_p, e_p) = \mathcal{N}^*((\phi, q), (\mathbf{e}, s)). \quad (3.48)$$

Chapter 4

Adjoint based analysis for MHD

As described at the outset, we want to apply the theory of adjoint based *a posteriori* error analysis (ABAPEA) developed so far to the equations of resistive incompressible magnetohydrodynamics (MHD). In this chapter, we develop specific theory to derive an adjoint problem and resulting error representation for the MHD equations. The MHD equations pose a host of challenges both analytically and numerically. In particular, the MHD equations are a rectangular system, and until now we have worked only with square systems. We must therefore define an adjoint directly to the weak form, in particular the exact penalty weak form. Furthermore, the complex nonlinear coupling between equations motivates a special ABAPEA theory for product spaces to clarify the discussion.

4.1 Exact penalty formulation and discretization for incompressible MHD

In this section we describe the nondimensionalized equations of incompressible stationary MHD, a stabilized weak form of the MHD system and a finite element method for its solution.

4.1.1 The MHD equations

The equations for stationary incompressible MHD in Ω are given by

$$-\frac{1}{\text{Re}}\Delta\mathbf{u} + (\mathbf{u} \cdot \nabla)\mathbf{u} + \nabla p - \kappa(\nabla \times \mathbf{b}) \times \mathbf{b} = \mathbf{f}, \quad (4.1a)$$

$$\nabla \cdot \mathbf{u} = 0, \quad (4.1b)$$

$$\frac{\kappa}{\text{Re}_m}\nabla \times (\nabla \times \mathbf{b}) - \kappa\nabla \times (\mathbf{u} \times \mathbf{b}) = \mathbf{0}, \quad (4.1c)$$

$$\nabla \cdot \mathbf{b} = 0, \quad (4.1d)$$

where the unknowns are the velocity \mathbf{u} , the magnetic field \mathbf{b} , and the pressure p . The nondimensionalized parameters are the fluid Reynolds number Re , Magnetic Reynolds number Re_m , and interaction parameter $\kappa = \text{Ha}^2\text{ReRe}_m$, where Ha is the Hartmann number. The source term \mathbf{f} is viewed as data to the problem. For $x \in \Omega$ we have $\mathbf{u}(x) \in \mathbb{R}^d$, $\mathbf{b}(x) \in \mathbb{R}^d$, $p(x) \in \mathbb{R}$ and $\mathbf{f}(x) \in \mathbb{R}^d$. We supplement the system (4.1) with boundary conditions,

$$\mathbf{u} = \mathbf{g}, \quad \text{on } \partial\Omega, \quad (4.2a)$$

$$\mathbf{b} \times \mathbf{n} = \mathbf{q} \times \mathbf{n}, \quad \text{on } \partial\Omega. \quad (4.2b)$$

Referring to (4.1), we observe there are $2d + 2$ and only $2d + 1$ unknowns [54]. Effectively enforcing the solenoidal constraint (4.1d) (an involution of the transient

MHD system) is an open area of research. Techniques include compatible discretizations [55, 53], vector potential [4, 56] and divergence cleaning [22, 43] as well as the exact penalty method [39, 35, 54]. In this thesis, we consider the exact penalty method which we further describe in §4.1.3.

4.1.2 Function spaces for the MHD system

The relevant subspaces of $\mathbf{H}^1(\Omega)$ needed to satisfy the boundary conditions (in the sense of the trace operator) are,

$$\mathbf{H}_0^1(\Omega) := \{\mathbf{w} \in \mathbf{H}^1 : \mathbf{w}|_{\partial\Omega} \equiv \mathbf{0}\}, \quad (4.3)$$

$$\mathbf{H}_\tau^1(\Omega) := \{\mathbf{w} \in \mathbf{H}^1 : (\mathbf{w} \times \mathbf{n})|_{\partial\Omega} \equiv \mathbf{0}\}. \quad (4.4)$$

We also define the product space,

$$\mathcal{P}(\Omega) := \mathbf{H}_0^1(\Omega) \times \mathbf{H}_\tau^1(\Omega) \times L^2(\Omega). \quad (4.5)$$

We also remark that for $d = 2$, we use the natural inclusion of $\mathbb{R}^2 \hookrightarrow \mathbb{R}^3$, $[v_1, v_2]^T \mapsto [v_1, v_2, 0]^T$ to define the operators $\nabla \times$ and \times . Thus for $\mathbf{v}, \mathbf{w} \in \mathbf{H}^1$, we have that

$$\nabla \times \mathbf{v} = \left(\frac{\partial v_y}{\partial x} - \frac{\partial v_x}{\partial y} \right) \hat{\mathbf{k}}, \quad \mathbf{v} \times \mathbf{w} = (v_x w_y - v_y w_x) \hat{\mathbf{k}}.$$

4.1.3 Exact penalty formulation

In this section we present the weak form of the stationary incompressible MHD system based on the exact penalty formulation. The exact penalty method requires that the domain Ω is bounded, convex and polyhedral. This ensures that $\mathbf{H}(\mathbf{curl}, \Omega) \cap \mathbf{H}(\mathbf{div}, \Omega)$ is continuously embedded in $\mathbf{H}^1(\Omega)$ [53]. We also assume homogeneous Dirichlet conditions, $\mathbf{g} = \mathbf{q} = \mathbf{0}$. Non-homogeneous boundary conditions can be dealt with through standard lifting arguments as discussed in

§4.3.3. The exact penalty weak problem corresponding to (4.1) and (4.2) is: find $U = (\mathbf{u}, \mathbf{b}, p) \in \mathcal{P}(\Omega)$ such that

$$\mathcal{N}_{EP}(U, V) = (\mathbf{f}, \mathbf{v}), \quad \forall V \in \mathcal{P}(\Omega), \quad (4.6)$$

where the nonlinear form \mathcal{N}_{EP} is defined for all $V = (\mathbf{v}, \mathbf{c}, q) \in \mathcal{P}(\Omega)$ by

$$\begin{aligned} \mathcal{N}_{EP}(U, V) &:= \frac{1}{R}(\nabla \mathbf{u}, \nabla \mathbf{v}) + (\mathbf{C}(\mathbf{u}), \mathbf{v}) - (p, \nabla \cdot \mathbf{v}) + (q, \nabla \cdot \mathbf{u}) \\ &+ \kappa(\mathcal{Y}(\mathbf{b}), \mathbf{v}) - \kappa(\mathcal{Z}(\mathbf{u}, \mathbf{b}), \mathbf{c}) \\ &+ \frac{\kappa}{\text{Re}_m}(\nabla \times \mathbf{b}, \nabla \times \mathbf{c}) + \frac{\kappa}{\text{Re}_m}(\nabla \cdot \mathbf{b}, \nabla \cdot \mathbf{c}), \end{aligned} \quad (4.7)$$

and the nonlinear operators are defined by

$$\mathbf{C}(\mathbf{u}) := (\mathbf{u} \cdot \nabla) \mathbf{u}, \quad (4.8a)$$

$$\mathcal{Y}(\mathbf{b}) := (\nabla \times \mathbf{b}) \times \mathbf{b}, \quad (4.8b)$$

$$\mathcal{Z}(\mathbf{u}, \mathbf{b}) := \nabla \times (\mathbf{u} \times \mathbf{b}). \quad (4.8c)$$

All except the last term in the weak form arise from multiplying (4.1a)-(4.1c) by test functions and performing integration by parts. The last term, $\frac{\kappa}{\text{Re}_m}(\nabla \cdot \mathbf{b}, \nabla \cdot \mathbf{c})$, effectively enforces the solenoidal involution (4.1d) since, assuming the aforementioned restrictions on the domain, there exists a function (see [39, 37]) $b_0 \in H^2(\Omega)$ such that

$$\nabla \cdot \nabla b_0 = \nabla \cdot \mathbf{b}, \text{ and } \nabla b_0 \in \mathbf{H}_\tau^1(\Omega). \quad (4.9)$$

Thus, we choose $V = (\mathbf{0}, \nabla b_0, 0)$ in (4.7) and use (B.5) so that (4.6) reduces to

$$(\nabla \cdot \mathbf{b}, \nabla \cdot \nabla b_0) = (\nabla \cdot \mathbf{b}, \nabla \cdot \mathbf{b}) = 0, \quad (4.10)$$

and hence (4.1d) is satisfied almost everywhere in Ω .

4.1.4 Finite element method

Additionally, our finite element space satisfies the Ladyzhenskaya-Babuška-Brezzi stability [12] condition for the velocity pressure pair, e.g. $\mathcal{P}_h(\Omega) = \mathbb{P}_h^2(\Omega) \times \mathbb{P}_h^1(\Omega) \times$

$\mathbb{P}_h^1(\Omega)$. Then the discrete problem to find an approximate solution $U_h = (\mathbf{u}_h, \mathbf{b}_h, p_h) \in \mathcal{P}_h(\Omega)$ to (4.7) is,

$$\mathcal{N}_{EP}(U_h, V_h) = (\mathbf{f}, \mathbf{v}_h) \quad \forall V_h \in \mathcal{P}_h(\Omega). \quad (4.11)$$

Note there is no restriction on the finite element space for \mathbf{b}_h , which is an advantage of this method. The well-posedness of the continuous and discrete problems are proven in [39].

4.1.5 Quantity of interest (QoI)

The goal of a numerical simulation is often to compute some functional of the solution, that is, the QoI. In particular, QoIs considered in this thesis have the generic form,

$$\text{QoI} = \int_{\Omega} \Psi \cdot U \, dx = (\Psi, U) \quad (4.12)$$

where $\Psi \in \mathbf{L}^2(\Omega) \times \mathbf{L}^2(\Omega) \times L^2(\Omega) \equiv [L^2(\Omega)]^{2d+1}$. For example in 2D, to compute the average of the y component of velocity u_y over a region $\Omega_c \subset \Omega$, set $\Psi = \frac{1}{|\Omega_c|}(0, \mathbb{1}_{\Omega_c}, 0, 0, 0)^T$, where $\mathbb{1}_S$ denotes the characteristic function over a set S . In the examples presented later, the QoIs physically represent quantities representative of the average flow rate, or the average induced magnetic field. We seek to compute error estimates in the QoI using duality arguments as presented in the following subsection.

4.2 Abstract *a posteriori* error analysis

In this section we consider an abstract variational setting for *a posteriori* analysis based on the ideas from [32, 25, 36, 5, 8] and already partially addressed in Chapters 2 and 3. Let \mathcal{W} be a Hilbert space with inner product $\langle \cdot, \cdot \rangle$ and let \mathcal{V} be a dense

subspace. We consider generic QoI as bounded linear functionals of the form,

$$Q(w) = \langle \psi, w \rangle,$$

where $\psi, w \in \mathcal{W}$. For example, in (4.12), $\langle \psi, u \rangle = (\Psi, U)$, the abstract inner product is represented by the L^2 inner product. We want to evaluate $Q(u)$ where u is the solution to the variational problem: find u in \mathcal{V} such that

$$\mathcal{N}(u, v) = \langle f, v \rangle, \quad \forall v \in \mathcal{V}, \quad (4.13)$$

and $\mathcal{N} : \mathcal{V} \times \mathcal{V} \rightarrow \mathbb{R}$ is linear in the second argument but may be nonlinear in the first argument. Throughout this section u refers to the true solution to (4.13). An example of such a variational problem is the exact penalty problem as described in §4.1.3. Given a numerical approximation $u_h \in \mathcal{V}_h$, in some finite dimensional subspace $\mathcal{V}_h \subset \mathcal{V}$, we define the error as $e = u - u_h$. The aim of the *a posteriori* analysis is to compute the error in the QoI, $Q(u) - Q(u_h) = \langle \psi, u \rangle - \langle \psi, u_h \rangle = \langle \psi, e \rangle$. For nonlinear forms, the choice of an adjoint form is not straightforward. However, a common choice useful for various kinds of analysis is based on linearization [50, 49, 16, 15, 33]. Indeed, this is related the definition in Theorem 3.1.2 in a way that will be made clear in the following discussion.

To closely mimic the exact penalty problem (4.6), let $\mathcal{V} = \prod_{i=1}^n \mathcal{V}_i$ be a product space of Hilbert spaces and $\mathcal{W} = \prod_{i=1}^n \mathcal{W}_i$ such that \mathcal{V}_i is a dense subspace of \mathcal{W}_i for all i . These spaces are defined on a domain so that $\mathcal{V}_i = \mathcal{V}_i(\Omega)$, and $\mathcal{W}_i = \mathcal{W}_i(\Omega)$, with $\Omega \subset \mathbb{R}^d$. We now define $\mathcal{N} : \mathcal{V} \times \mathcal{V} \rightarrow \mathbb{R}$ by

$$\mathcal{N}(u, v) = \sum_{i=1}^m \langle N_i(u), v_{\ell_i} \rangle + a(u, v), \quad (4.14)$$

where $a(u, v)$ is a bilinear form and $\ell_i \in \{1, \dots, n\}$ and $N_i : \mathcal{V} \rightarrow \mathcal{W}_{\ell_i}$. Note that (4.7) is a particular case of (4.14). For a solution/approximation pair (u/u_h) , define the matrix $\overline{\mathcal{J}}$, by

$$\overline{\mathcal{J}}_{ij} = \int_0^1 \frac{\partial N_i}{\partial u_j}(su + (1-s)u_h) ds, \quad (4.15)$$

Chapter 4. Adjoint based analysis for MHD

where $\frac{\partial N_i}{\partial u_j}(\cdot)$ denotes the partial derivative of N_i with respect to the argument u_j .

Define the linearized operator \bar{N}_i for $w \in \mathcal{V}$ by

$$\begin{aligned}\bar{N}_i w &= \int_0^1 \frac{\partial N_i}{\partial u}(su + (1-s)u_h) ds \cdot w \\ &= \sum_{j=1}^n \int_0^1 \frac{\partial N_i}{\partial u_j}(su + (1-s)u_h) ds w_j = \sum_{j=1}^n \bar{\mathcal{J}}_{ij} w_j.\end{aligned}$$

Now since each \bar{N}_i is linear, we may define the bilinear forms,

$$\bar{v}_i(u, v) = \langle \bar{N}_i u, v_{\ell_i} \rangle = \left\langle \sum_{j=1}^n \bar{\mathcal{J}}_{ij} u_j, v_{\ell_i} \right\rangle = \sum_{j=1}^n \langle \bar{\mathcal{J}}_{ij} u_j, v_{\ell_i} \rangle.$$

Define $\bar{v}_i^*(v, w) = \bar{v}_i(w, v)$, adjoint operators $\bar{\mathcal{J}}_{ij}^*$ to $\bar{\mathcal{J}}_{ij}$ satisfying

$$\langle \bar{\mathcal{J}}_{ij} w, v \rangle = \langle w, \bar{\mathcal{J}}_{ij}^* v \rangle \quad (4.16)$$

for $w \in \mathcal{V}_j$ and $v \in \mathcal{V}_{\ell_i}$ and $a^*(w, v) := a(v, w)$, as per definition (2.10). With these definitions, the adjoint bilinear weak form is,

$$\bar{\mathcal{N}}^*(\phi, w) = \sum_{i=1}^m \bar{v}_i^*(\phi, v) + a^*(\phi, v) = \sum_{i=1}^m \sum_{j=1}^n \langle v_j, \bar{\mathcal{J}}_{ij}^* \phi_{\ell_i} \rangle + a^*(\phi, v). \quad (4.17)$$

Then if ϕ solves the dual problem,

$$\bar{\mathcal{N}}^*(\phi, v) = \langle \psi, v \rangle, \quad \forall v \in \mathcal{V}, \quad (4.18)$$

we then have the following abstract error representation.

Theorem 4.2.1. *The error in a QoI represented by $Q(u) = \langle \psi, u \rangle$ is compatible as $\langle \psi, e \rangle = \langle f, \phi \rangle - \mathcal{N}(u_h, \phi)$.*

Proof. Unpacking the definitions,

$$\begin{aligned}
 \langle \psi, e \rangle &= \overline{\mathcal{N}}^*(\phi, e) = \sum_{i=1}^m \sum_{j=1}^n \langle e_j, \overline{\mathcal{J}}_{ij}^* \phi_{\ell_i} \rangle + a^*(\phi, e) \\
 &= \sum_{i=1}^m \sum_{j=1}^n \langle \overline{\mathcal{J}}_{ij} e_j, \phi_{\ell_i} \rangle + a(e, \phi) = \sum_{i=1}^m \langle \overline{N}_i e, \phi_{\ell_i} \rangle + a(e, \phi) \\
 &= \sum_{i=1}^m \langle N_i(u) - N_i(u_h), \phi_{\ell_i} \rangle + a(u, \phi) - a(u_h, \phi) \\
 &= \sum_{i=1}^m \langle N_i(u), \phi_{\ell_i} \rangle + a(u, \phi) - \sum_{i=1}^m \langle N_i(u_h), \phi_{\ell_i} \rangle - a(u_h, \phi) \\
 &= \mathcal{N}(u, \phi) - \mathcal{N}(u_h, \phi) = (f, \phi) - \mathcal{N}(u_h, \phi).
 \end{aligned}$$

□

The main takeaway of this theorem is that computing the adjoint to a nonlinear form is reduced to computing the adjoint for the averaged entries, $\overline{\mathcal{J}}_{ij}$.

4.3 *A posteriori* error estimate applied to MHD

The analysis in §4.2 applies directly to the MHD equations. The duality pairing of the last section is represented by the $[L^2(\Omega)]^{2d+1}$ inner product (\cdot, \cdot) . The linear and nonlinear terms in the exact penalty weak form (4.6) are mapped to match (4.14). The mapping between the abstract formulation and MHD equation is shown in Table 4.1.

For the exact penalty weak form, we have that

$$\mathcal{N}_{EP}(U, V) = \sum_{i=1}^3 (N_{EP,i}(U), V_{\ell_i}) + a_{EP}(U, V), \quad (4.19)$$

where

$$\begin{aligned}
 (N_{EP,1}(U), V_2) &= (\mathcal{Z}(\mathbf{u}, \mathbf{b}), \mathbf{c}), \\
 (N_{EP,2}(U), V_1) &= (\mathcal{Y}(\mathbf{b}), \mathbf{v}), \\
 (N_{EP,3}(U), V_1) &= (\mathcal{C}(\mathbf{u}), \mathbf{v}),
 \end{aligned} \quad (4.20)$$

Abstract	MHD
\langle , \rangle	$(,)$
m	3
\mathcal{N}	\mathcal{N}_{EP}
u	U
v	V
N_i	$N_{EP,i}$

(a)

Abstract	MHD
$\langle f, v \rangle$	(\mathbf{f}, \mathbf{v})
u_1	$U_1 \equiv \mathbf{u}$
u_2	$U_2 \equiv \mathbf{b}$
u_3	$U_3 \equiv p$
v_1	$V_1 \equiv \mathbf{v}$
v_2	$V_2 \equiv \mathbf{c}$

(b)

Abstract	MHD
v_3	$V_3 \equiv q$
$\overline{\mathcal{J}}_{11}^*$	$\overline{\mathcal{Z}}_{\mathbf{u}}^*$
$\overline{\mathcal{J}}_{12}^*$	$\overline{\mathcal{Z}}_{\mathbf{b}}^*$
$\overline{\mathcal{J}}_{21}^*$	$\overline{\mathcal{Y}}^*$
$\overline{\mathcal{J}}_{31}^*$	$\overline{\mathcal{C}}^*$
a	a_{EP}

(c)

Table 4.1: Mapping between the abstract framework in §4.2 and the MHD equation in §4.3. \mathcal{N}_{EP} is given in (4.19), $N_{EP,i}$ in (4.20), a_{EP} in (4.21) and $\overline{\mathcal{Z}}_{\mathbf{u}}^*$, $\overline{\mathcal{Z}}_{\mathbf{b}}^*$, $\overline{\mathcal{Y}}^*$, $\overline{\mathcal{C}}^*$ are given in (4.22).

$\mathcal{Z}, \mathcal{Y}, \mathcal{C}$ are in turned defined in (4.8), and

$$\begin{aligned}
 a_{EP}(U, V) &= \frac{1}{R}(\nabla \mathbf{u}, \nabla \mathbf{v}) - (p, \nabla \cdot \mathbf{v}) + (q, \nabla \cdot \mathbf{u}) \\
 &\quad + \frac{\kappa}{\text{Re}_m}(\nabla \times \mathbf{b}, \nabla \times \mathbf{c}) + \frac{\kappa}{\text{Re}_m}(\nabla \cdot \mathbf{b}, \nabla \cdot \mathbf{c}).
 \end{aligned} \tag{4.21}$$

The entries $\overline{\mathcal{J}}_{11}^* V_2 = \overline{\mathcal{Z}}_{\mathbf{u}}^*$, $\overline{\mathcal{J}}_{12}^* V_2 = \overline{\mathcal{Z}}_{\mathbf{b}}^*$, $\overline{\mathcal{J}}_{21}^* V_1 = \overline{\mathcal{Y}}^* \mathbf{v}$ and $\overline{\mathcal{J}}_{31}^* V_1 = \overline{\mathcal{C}}^* \mathbf{v}$ are,

$$\begin{aligned}
 \overline{\mathcal{Z}}_{\mathbf{u}}^* \mathbf{c} &= \frac{1}{2}(\mathbf{u} + \mathbf{u}_h) \times (\nabla \times \mathbf{c}), \\
 \overline{\mathcal{Z}}_{\mathbf{b}}^* \mathbf{c} &= -\frac{1}{2}(\mathbf{b} + \mathbf{b}_h) \times (\nabla \times \mathbf{c}), \\
 \overline{\mathcal{Y}}^* \mathbf{v} &= \frac{1}{2}(-(\nabla \times (\mathbf{b} + \mathbf{b}_h) \times \mathbf{v}) + \nabla \times ((\mathbf{b} + \mathbf{b}_h) \times \mathbf{v})), \\
 \overline{\mathcal{C}}^* \mathbf{v} &= \frac{1}{2}((\nabla \mathbf{u} + \nabla \mathbf{u}_h)^T \mathbf{v} - ((\mathbf{u} + \mathbf{u}_h) \cdot \nabla) \mathbf{v}) - (\nabla \cdot (\mathbf{u} + \mathbf{u}_h)) \mathbf{v},
 \end{aligned} \tag{4.22}$$

while the remaining $\overline{\mathcal{J}}_{ij}^*$ entries are zero. The details of the derivation are given in §4.5.1.

4.3.1 Weak form of adjoint for incompressible MHD

We are now prepared to pose a weak adjoint problem corresponding to exact penalty primal problem (4.6). Based on (4.19), (4.22) and (4.18), The weak dual problem is

therefore be stated as: find $\Phi = (\phi, \boldsymbol{\beta}, \pi) \in \mathcal{P}(\Omega)$ such that

$$\overline{\mathcal{N}}_{EP}^*(\Phi, V) = (\Psi, V), \quad \forall V \in \mathcal{P}(\Omega) \quad (4.23)$$

with

$$\begin{aligned} \overline{\mathcal{N}}_{EP}^*(\Phi, V) &= \frac{1}{\text{Re}} (\nabla \phi, \nabla \mathbf{v}) + (\overline{\mathcal{C}}^* \phi, \mathbf{v}) + (\nabla \cdot \mathbf{v}, \pi) - (\nabla \cdot \phi, q) \\ &+ \frac{\kappa}{\text{Re}_m} (\nabla \times \boldsymbol{\beta}, \nabla \times \mathbf{c}) + \frac{\kappa}{\text{Re}_m} (\nabla \cdot \boldsymbol{\beta}, \nabla \cdot \mathbf{c}) \\ &- \kappa (\overline{\mathcal{Y}}^* \phi, \mathbf{c}) - \kappa (\overline{\mathcal{Z}}_{\mathbf{u}}^* \boldsymbol{\beta}, \mathbf{v}) - \kappa (\overline{\mathcal{Z}}_{\mathbf{b}}^* \boldsymbol{\beta}, \mathbf{c}). \end{aligned} \quad (4.24)$$

The forms of the linear operators $\overline{\mathcal{C}}^*$, $\overline{\mathcal{Y}}^*$, $\overline{\mathcal{Z}}_{\mathbf{u}}^*$ and $\overline{\mathcal{Z}}_{\mathbf{b}}^*$ are given in (4.22). We discuss the well-posedness of the adjoint weak form in §4.5.2.

4.3.2 Error representation

In order to discuss error representation we need to the following definitions

Definition 4.3.1. Define the monolithic error by $E = [\mathbf{e}_{\mathbf{u}}, \mathbf{e}_{\mathbf{b}}, e_p]^T$ with component errors

$$\mathbf{e}_{\mathbf{u}} = \mathbf{u} - \mathbf{u}_h, \quad \mathbf{e}_{\mathbf{b}} = \mathbf{b} - \mathbf{b}_h, \quad e_p = p - p_h. \quad (4.25)$$

We have the following error representation.

Theorem 4.3.1 (Error representation for exact penalty). *For a given QoI represented by $\Psi = [\boldsymbol{\psi}_{\mathbf{u}}, \boldsymbol{\psi}_{\mathbf{b}}, \psi_p]^T$, the error in the numerical approximation of the QoI satisfies*

$$\begin{aligned} (\Psi, E) &= (\mathbf{f}, \phi) - \left[\frac{1}{\text{Re}} (\nabla \mathbf{u}_h, \nabla \phi) + ((\mathbf{u}_h \cdot \nabla) \mathbf{u}_h, \phi) \right. \\ &\quad - (p_h, \nabla \cdot \phi) + \kappa ((\nabla \times \mathbf{b}_h) \times \mathbf{b}_h, \phi) + (\nabla \cdot \mathbf{u}_h, \pi) \\ &\quad + \frac{\kappa}{\text{Re}_m} (\nabla \times \mathbf{b}_h, \nabla \times \boldsymbol{\beta}) + \kappa (\nabla \times (\mathbf{u}_h \times \mathbf{b}_h), \boldsymbol{\beta}) \\ &\quad \left. + \frac{\kappa}{\text{Re}_m} (\nabla \cdot \mathbf{b}_h, \nabla \cdot \boldsymbol{\beta}) \right]. \end{aligned}$$

Proof. By Theorem 4.2.1,

$$(\Psi, E) = \overline{\mathcal{N}}_{EP}^*(\Phi, E) = \mathcal{N}_{EP}(U, \Phi) - \mathcal{N}_{EP}(U_h, \Phi) = (\mathbf{f}, \boldsymbol{\phi}) - \mathcal{N}_{EP}(U_h, \Phi).$$

□

4.3.3 Non-homogeneous boundary conditions for the MHD system

The analysis above easily extends to the case of non-homogeneous boundary conditions, i.e. when \mathbf{g} or $\mathbf{q} \times \mathbf{n}$ are not identically zero. First assume that the numerical solution U^h that satisfies the non-homogeneous conditions exactly. That is, $\mathbf{u} = \mathbf{u}_h = \mathbf{g}$ and $\mathbf{b} \times \mathbf{n} = \mathbf{b}_h \times \mathbf{n} = \mathbf{q} \times \mathbf{n}$ on $\partial\Omega$. Then, although neither the true solution U nor the numerical solution U^h belong to $\mathcal{P}(\Omega)$, yet the error, $\mathbf{E} = U - U^h$, satisfies homogeneous boundary conditions and hence belongs to $\mathcal{P}(\Omega)$. Thus, the error analysis in the previous section applies directly in this case.

Now, if U_h belongs to $\mathcal{P}_h(\Omega)$, then in general U_h does not satisfy the non-homogeneous boundary conditions exactly. Hence we consider the splitting of the numerical solutions as,

$$U_h = U_h^0 + U^d, \tag{4.26}$$

where $U_h^0 \in \mathcal{P}_h(\Omega)$ solves,

$$\mathcal{N}_{EP}(U_h, V_h) = \mathcal{N}_{EP}(U_h^0 + U^d, V_h) = (F, V_h), \quad \forall V_h \in \mathcal{P}_h(\Omega), \tag{4.27}$$

and U^d is a known function that satisfies the non-homogeneous boundary conditions accurately. That is, the unknown is now U_h^0 and the numerical solution U_h is formed through the sum in (4.26). In this thesis the function U^d is approximated through a finite element space of much higher dimension than $\mathcal{P}_h(\Omega)$ to capture the boundary conditions accurately.

4.3.4 Error estimate and contributions

The error representation in Theorem 4.3.1 requires the exact solution $\Phi = (\boldsymbol{\phi}, \boldsymbol{\beta}, \pi) \in \mathcal{P}(\Omega)$. Moreover, the adjoint weak form (4.24) is linearized around the true solution U and the approximate solution U_h . In practice, the adjoint solution itself must be approximated in a finite element space $\mathcal{W}^h \subset \mathcal{P}(\Omega)$ and is linearized only around the numerical solution. These approximations lead to an error estimate from the error representation 4.3.1. Let this estimate be denoted by η_{EP} . That is, $\eta_{EP} \approx (\Psi, E)$ where,

$$\eta_{EP} = E_{mom} + E_{con} + E_M, \quad (4.28)$$

where,

$$\begin{aligned} E_{mom} = & (\mathbf{f}, \boldsymbol{\phi}_h) - \left(\frac{1}{\text{Re}} (\nabla \mathbf{u}_h, \nabla \boldsymbol{\phi}_h) + (\mathbf{u}_h \cdot \nabla \mathbf{u}_h, \boldsymbol{\phi}_h) - (p_h, \nabla \cdot \boldsymbol{\phi}_h) \right. \\ & \left. + \kappa ((\nabla \times \mathbf{b}_h) \times \mathbf{b}_h, \boldsymbol{\phi}_h) \right), \end{aligned} \quad (4.29)$$

$$E_{con} = -(\nabla \cdot \mathbf{u}_h, \pi_h),$$

$$E_M = -\frac{\kappa}{\text{Re}_m} (\nabla \times \mathbf{b}_h, \nabla \times \boldsymbol{\beta}_h) + \kappa (\nabla \times (\mathbf{u}_h \times \mathbf{b}_h), \boldsymbol{\beta}_h) - \frac{\kappa}{\text{Re}_m} (\nabla \cdot \mathbf{b}_h, \nabla \cdot \boldsymbol{\beta}_h).$$

Here E_{mom} , E_{con} and E_M represent the momentum error contribution, the continuity error contribution and the magnetic error contribution respectively.

To obtain an accurate error estimate we choose \mathcal{W}^h to be of much higher dimension than $\mathcal{P}_h(\Omega)$ as is standard in adjoint based *a posteriori* error estimation [27, 32, 25, 19, 20, 27, 21, 14, 9]. Moreover, the inaccuracy caused by substituting the numerical solution in place of true solution in the adjoint weak form is shown to decrease in the limit of refined discretization [27].

4.4 Numerical Experiments

In this section we present numerical results to verify the accuracy of the error estimate (4.28) and the utility of the error contributions in (4.29). We present two numerical examples here, the Hartmann problem §4.4.1 and the magnetic lid driven cavity §4.4.2. Since there is no closed form solution for the magnetic lid driven cavity, we use a reference high order/fine mesh to get a good estimate for the true error. All the following computations are carried out using the finite element package `Dolfin` in the `FEniCS` suite [6, 47, 48]. We use the built-in LU solver for the linear problems in the Newton iteration, as well as the linearized adjoint problem.

For all experiments, we choose different polynomial orders of Lagrange spaces for the product space $\mathcal{P}_h(\Omega)$ and ensure that the adjoint space \mathcal{W}_h has a higher polynomial degree. The computational domain for all problems is chosen to be a unit length square, $\Omega := [-\frac{1}{2}, \frac{1}{2}]^2 \subset \mathbb{R}^2$. The mesh is a simplicial uniform mesh with the total number of 2D elements, $\text{Elem.} = n_e \times n_e$. We again make use of the effectivity ratio, Eff. , as defined in (3.21) now for the estimator η_{EP} given by (4.28).

4.4.1 Hartmann flow in 2D

Our first results concern the so-called Hartmann problem [59]. This problem models the flow of a conducting fluid in a channel. In this case we consider a square channel, as described in the beginning of the section. This problem admits an analytic solution [54], $\mathbf{u} = (u_x, 0)$, $\mathbf{b} = (B_x, 1)$, p where

$$u_x(y) = \frac{G \operatorname{Re}(\cosh(\text{Ha}/2) - \cosh(\text{Ha} y))}{2\text{Ha} \sinh(\text{Ha}/2)}, \quad (4.30a)$$

$$B_x(y) = \frac{G(\sinh(\text{Ha} y) - 2 \sinh(\text{Ha}/2)y)}{2\kappa \sinh(\text{Ha}/2)}, \quad (4.30b)$$

$$p(x) = -Gx - \kappa B_x^2/2, \quad (4.30c)$$

Chapter 4. Adjoint based analysis for MHD

and $G = -\frac{dp}{dx}$ is an arbitrary pressure drop that we choose to normalize maximum velocity $u_x(y)$ to 1.

Problem parameters and QoI

The values of the nondimensionalized constants are chosen as follows: $\text{Re} = 16$, $\text{Re}_m = 16$, $\kappa = 1$ which produce a Hartmann number of $\text{Ha} = 16$. The QoI is chosen as the average velocity across the flow over a slice. To this end, define

$$\Omega_c := \left[-\frac{1}{4}, \frac{1}{2}\right] \times \left[-\frac{1}{4}, \frac{1}{4}\right] \quad (4.31)$$

and consequently $\mathbb{1}_{\Omega_c}$ the characteristic function on Ω_c . The monolithic quantity of interest Ψ as in Theorem 4.3.1 is chosen to be $\Psi = \left[\mathbb{1}_{\Omega_c}, 0, 0, 0, 0\right]^T$. The QoI thus reduces to

$$(\Psi, U) = (\mathbb{1}_{\Omega_c}, u_x). \quad (4.32)$$

This has a physical interpretation of the capturing the flow rate across this slice of the channel, Ω_c .

Numerical results and discussion

Error contributions and effectivites using different order polynomial spaces are presented in Table 4.2, Table 4.3, Table 4.4, and Table 4.5. Effectively ratio in tables 4.2 and 4.3 is quite close to 1 indicating the accuracy of the error estimate. The error estimate in Table 4.4 is not as accurate due to linearization error incurred by replacing the true solution by the approximate solution in the definition of the adjoint as discussed in the introduction of this section and in Remark 3.1.1. This may be verified by linearizing the adjoint weak form around both the true (which we know for this example) and the approximate solutions. These results are shown in Table 4.5 and now the error estimate is again accurate. We believe the linearization error is

especially apparent in this example since the error in the QoI is quite small compared to the other numerical experiments. In particular, approximations in solutions of the adjoint problem will be more apparent.

We remark that for the lowest order tuple $(\mathbb{P}^2, \mathbb{P}^1, \mathbb{P}^1)$ for the variables $(\mathbf{u}, \mathbf{b}, p)$ in Table 4.2, the error is largely dominated by the contributions E_{con} and E_M . We greatly reduce the error in E_M by using a higher order space for \mathbf{b} as demonstrated in Table 4.3. However, this does not reduce the magnitude of the total error much (about 5%) which is still dominated by the contribution E_{con} . The contribution E_{con} is not significantly affected by the finite dimensional space for \mathbf{b} . Now finally, if we refine all three variables, Table 4.4 shows that the total error drops by two orders of magnitude.

2D Elem.	True Error	Eff.	E_{mom}	E_{con}	E_M
1600	2.76e-04	1.00	4.53e-06	-2.28e-04	5.00e-04
6400	6.98e-05	1.00	1.29e-06	-6.23e-05	1.31e-04
14400	3.11e-05	1.00	6.05e-07	-2.86e-05	5.91e-05
25600	1.75e-05	1.00	3.49e-07	-1.63e-05	3.35e-05

Table 4.2: Error in $(u_x, \mathbb{1}_{\Omega_c})$ for the Hartmann problem §4.4.1, with $\mathbb{1}_{\Omega_c} = [-\frac{1}{4}, \frac{1}{2}] \times [-\frac{1}{4}, \frac{1}{4}]$. The finite dimensional space here is $(\mathbb{P}^2, \mathbb{P}^1, \mathbb{P}^1)$ for $(\mathbf{u}, \mathbf{b}, p)$.

2D Elem.	True Error	Eff.	E_{mom}	E_{con}	E_M
1600	-2.25e-04	1.02	1.08e-06	-2.27e-04	-4.79e-06
6400	-6.13e-05	1.04	1.04e-06	-6.23e-05	-2.18e-06
14400	-2.81e-05	1.04	5.98e-07	-2.86e-05	-1.13e-06
25600	-1.60e-05	1.04	3.76e-07	-1.64e-05	-6.81e-07

Table 4.3: Error in $(u_x, \mathbb{1}_{\Omega_c})$ for the Hartmann problem §4.4.1. The finite dimensional space here is $(\mathbb{P}^2, \mathbb{P}^2, \mathbb{P}^1)$ for $(\mathbf{u}, \mathbf{b}, p)$.

2d Elem.	True Error	Eff.	E_{mom}	E_{con}	E_M
1600	1.23e-06	1.21	3.97e-07	-4.15e-06	5.24e-06
6400	1.46e-07	1.47	9.23e-08	-5.07e-07	6.29e-07
14400	4.97e-08	1.63	3.84e-08	-1.40e-07	1.83e-07
25600	2.47e-08	1.73	2.07e-08	-5.44e-08	7.64e-08

Table 4.4: Error in $(u_x, \mathbb{1}_{\Omega_c})$ for the Hartmann problem §4.4.1. The finite dimensional space here is $(\mathbb{P}^3, \mathbb{P}^2, \mathbb{P}^2)$ for $(\mathbf{u}, \mathbf{b}, p)$. Here, we approximate the true solution with the computed solution which results in linearization error as described in Remark 3.1.1. For this accurate a solution, this deteriorates the quality of the estimate which in turn results in a effectivity further from 1. This is confirmed in Table 4.5 where we use the true solution and the effectivity is again close to 1.

2d Elem.	True Error	Eff.	E_{mom}	E_{con}	E_M
1600	1.23e-06	1.00	2.75e-07	-4.39e-06	5.34e-06
6400	1.46e-07	1.00	5.97e-08	-5.60e-07	6.46e-07
14400	4.97e-08	1.00	2.35e-08	-1.63e-07	1.89e-07
25600	2.47e-08	1.00	1.22e-08	-6.65e-08	7.90e-08

Table 4.5: Error in $(u_x, \mathbb{1}_{\Omega_c})$ for the Hartmann problem, §4.4.1. The finite dimensional space here is $(\mathbb{P}^3, \mathbb{P}^2, \mathbb{P}^2)$ for $(\mathbf{u}, \mathbf{b}, p)$. No linearization error is present here because we use the true solution in the definition of the adjoint.

4.4.2 Magnetic Lid Driven Cavity

Regularization and solution method

The magnetic lid driven cavity is another common benchmark problem for verifying MHD codes [54, 57]. However, the standard lid velocity is discontinuous and therefore has at most $H^{1/2-\varepsilon}$ regularity in 2D with $\varepsilon > 0$. By the converse of the trace theorem and the Sobolev inequality [26, 13], the solution u_x cannot obtain H^1 regularity on the interior. Indeed, in this situation, we do not even have well posedness of the primal problem, so there is not real hope for error analysis. This issue has been addressed in a purely fluid context [40, 44]. In both cases, a regularization of the lid velocity is proposed to mitigate theoretical issues (in the former) and the ability

to achieve higher Reynolds numbers (in the latter). In this work, we use a similar regularization to the one proposed in [44], a polynomial regularization of the lid velocity,

$$u_{top}(x) = C \left(x - \frac{1}{2}\right)^2 \left(x + \frac{1}{2}\right)^2,$$

with C chosen such that

$$\int_{-1/2}^{1/2} u_{top}(x) dx = 1.$$

The boundary conditions are imposed as $\mathbf{g}(x, 0.5) = [u_{top}, 0]^T$ on the top face and zero on the rest of the boundary. We specify the boundary conditions on the magnetic field $\mathbf{b} \times \mathbf{n}$ by setting $\mathbf{q} = [-1, 0]^T$ so that $\mathbf{b} \times \mathbf{n} = [-1, 0] \times \mathbf{n}$ on $\partial\Omega$. To get a qualitative measure of the validity of the regularized problem, we show plots of the velocity profile for a fixed Reynolds number $\text{Re} = 5000$ and varying magnetic Reynolds numbers Re_m in Figure 4.1. These plots are qualitatively similar to Figure 1 in [54] (for which an un-regularized lid velocity is used), which gives us a good indication that the regularized version produces qualitatively similar features.

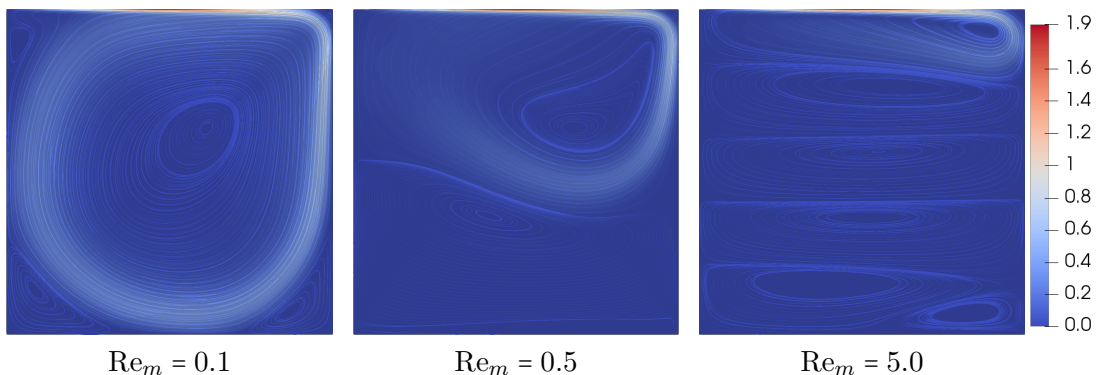


Figure 4.1: Plots of the $\|\mathbf{u}\|_{\mathbb{R}^d}$ for the lid driven cavity §4.4.2 using a normalization on the lid velocity over a variety of magnetic Reynolds numbers, Re_m . The other nondimensionalized parameters are $\text{Re} = 5000, \kappa = 1$ for all of these plots.

Furthermore, since high Re flows provide difficulties for the continuous Galerkin method [23], we use a homotopic sequence of initial guesses to achieve high Re .

Indeed, we run the problem for a moderate value of $\text{Re} = 200$ for example, and then use the solution produced by the solver as the initial guess for a larger value e.g. $\text{Re} = 1000$ until we have achieved the desired value. Figure 4.2 shows the intermediate values in this sequence to solve a problem with $\text{Re} = 1000$.

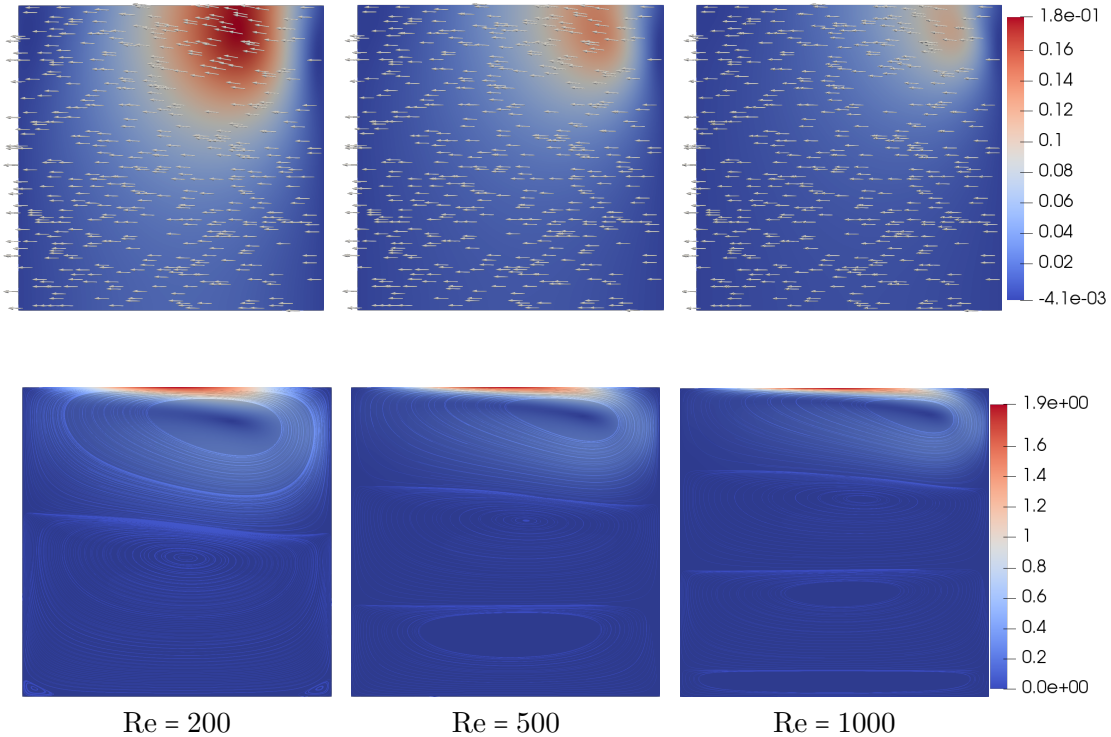


Figure 4.2: Demonstrating the homotopy parameter strategy to achieve high fluid Reynolds numbers as described in §4.4.2. The other nondimensionalized parameters $\text{Re}_m = 5.0, \kappa = 1$ for all of these plots. The top row is colored according the b_y and with the arrows representing the vector \mathbf{b} . The bottom row is colored according to the magnitude of \mathbf{u} , with added streamlines.

Results for $\text{QoI}(u_x)$

We take the same QoI as for the Hartmann problem although now with

$$\Omega_c := \left[-\frac{1}{4}, \frac{1}{4}\right] \times \left[-\frac{1}{2}, 0\right], \quad (4.33)$$

so that the QoI $(\Psi, U) = (\mathbb{1}_{\Omega_c}, u_x)$ has the physical interpretation of capturing the re-circulation in the lower half of the box. Since there is no analytic solution for this problem, we compute a solution on a 400×400 mesh in the space $(\mathbb{P}^3, \mathbb{P}^2, \mathbb{P}^2)$ for $(\mathbf{u}, \mathbf{b}, p)$. We consider the QoI obtained from this “overkill” solution as a the true solution to compute the error in the denominator of the effectivity ratio (3.21).

The effectivity ratio and error contributions for various values of Re are shown in Tables 4.6, 4.7, , 4.8 and 4.9. We note that the error estimate is accurate in all cases with effectivity ratios close to 1.

In terms of error contributions, for the lowest order cases of $(\mathbb{P}^2, \mathbb{P}^1, \mathbb{P}^1)$, both Re = 2000 and Re = 1000 in have a fairly balanced distribution of error between the components as seen in Tables 4.6 and 4.8. Similarly to the Hartmann problem, when use a higher order space space for \mathbf{b} , namely \mathbb{P}^2 , the contribution E_M decreases by several orders of magnitude, but the overall error remains dominated by E_{con} and E_{mom} . This is seen in 4.7 for Re = 1000 and 4.9 for Re = 2000. In particular, since the error was initially dominated by E_{mom} and E_{con} , we do not see any significant improvement in the true error. ABAPEA therefore, by exposing error contributions, can help inform the choice of finite dimensional spaces for the different DOFs.

2d Elem.	True Error	Eff.	E_{mom}	E_{con}	E_M
1600	5.02e-04	0.97	8.95e-05	2.21e-04	1.75e-04
3600	1.61e-04	0.96	2.19e-05	5.27e-05	8.06e-05
6400	7.20e-05	0.98	8.65e-06	1.58e-05	4.60e-05
10000	4.02e-05	0.99	4.02e-06	6.06e-06	2.96e-05

Table 4.6: error in $(u_x, \mathbb{1}_{\Omega_c})$ for the lid driven cavity §4.4.2. The finite dimensional space here is $(\mathbb{P}^2, \mathbb{P}^1, \mathbb{P}^1)$ for $(\mathbf{u}, \mathbf{b}, p)$. We use an overkill solution on a $400 \times 400 = 160000$ element mesh and $(\mathbb{P}^3, \mathbb{P}^2, \mathbb{P}^2)$ elements. The parameters are Re = 1000, $Re_m = 0.4$, $\kappa = 1$.

Chapter 4. Adjoint based analysis for MHD

2d Elem.	True Error	Eff.	E_{mom}	E_{con}	E_M
1600	3.17e-04	0.99	9.36e-05	2.20e-04	-6.79e-07
3600	7.92e-05	0.95	2.27e-05	5.28e-05	-1.24e-07
6400	2.58e-05	0.96	8.95e-06	1.58e-05	-3.79e-08
10000	1.05e-05	0.97	4.14e-06	6.08e-06	-1.52e-08

Table 4.7: Error in $(u_x, \mathbb{1}_{\Omega_c})$ for the lid driven cavity §4.4.2. The finite dimensional space here is $(\mathbb{P}^2, \mathbb{P}^2, \mathbb{P}^1)$ for $(\mathbf{u}, \mathbf{b}, p)$. We use an overkill solution on a $400 \times 400 = 160000$ element mesh and $(\mathbb{P}^3, \mathbb{P}^2, \mathbb{P}^2)$ elements. The parameters are $\text{Re} = 1000, \text{Re}_m = 0.4, \kappa = 1$.

2d Elem.	True Error	Eff.	E_{mom}	E_{con}	E_M
1600	6.64e-04	1.08	2.83e-04	4.27e-04	6.81e-06
3600	2.00e-04	0.95	4.34e-05	1.37e-04	9.07e-06
6400	7.00e-05	0.95	1.49e-05	4.37e-05	7.71e-06
10000	3.06e-05	0.96	6.94e-06	1.68e-05	5.68e-06

Table 4.8: Error in $(u_x, \mathbb{1}_{\Omega_c})$ for the lid driven cavity §4.4.2. The finite dimensional space here is $(\mathbb{P}^2, \mathbb{P}^1, \mathbb{P}^1)$ for $(\mathbf{u}, \mathbf{b}, p)$. We use an overkill solution on a $400 \times 400 = 160000$ element mesh and $(\mathbb{P}^3, \mathbb{P}^2, \mathbb{P}^2)$ elements. The parameters are $\text{Re} = 2000, \text{Re}_m = 0.4, \kappa = 1$.

2d Elem.	True Error	Eff.	E_{mom}	E_{con}	E_M
1600	6.18e-04	1.12	2.78e-04	4.17e-04	-8.54e-07
3600	1.85e-04	0.98	4.24e-05	1.39e-04	-2.72e-07
6400	6.09e-05	0.97	1.47e-05	4.41e-05	-9.47e-08
10000	2.44e-05	0.98	6.90e-06	1.70e-05	-3.90e-08

Table 4.9: Error in $(u_x, \mathbb{1}_{\Omega_c})$ for the lid driven cavity §4.4.2. The finite dimensional space here is $(\mathbb{P}^2, \mathbb{P}^2, \mathbb{P}^1)$ for $(\mathbf{u}, \mathbf{b}, p)$. We use an overkill solution on a $400 \times 400 = 160000$ element mesh and $(\mathbb{P}^3, \mathbb{P}^2, \mathbb{P}^2)$ elements. The parameters are $\text{Re} = 2000, \text{Re}_m = 0.4, \kappa = 1$.

Results for $\text{QoI}(b_y)$

We take the $\text{QoI } \Psi = [0, 0, 0, \mathbb{1}_{\Omega_c}, 0]^T$ where now

$$\Omega_c := \left[-\frac{1}{4}, \frac{1}{4}\right] \times \left[0, \frac{1}{2}\right], \quad (4.34)$$

so that the QoI $(\Psi, U) = (\mathbb{1}_{\Omega_c}, b_y)$ gives a measure of the induced magnetic field in the upper middle half of the box. See Figure 4.2 for plots of the induced field b_y as a function of Reynolds number Re .

The effectivity ratio and error contributions for $Re = 1000$ and $Re = 2000$ are shown in Tables 4.10, 4.11, 4.12 and 4.13. The error estimate η_{EP} is deemed accurate since all effectivity ratios are close to 1.

We first study the lowest order case, namely using the space $(\mathbb{P}^2, \mathbb{P}^1, \mathbb{P}^1)$ for $(\mathbf{u}, \mathbf{b}, p)$ in Table 4.10 where $Re = 1000$ and Table 4.12 where $Re = 2000$. For both $Re = 2000$ and $Re = 1000$, the error contributions are not drastically different in magnitude, and become even more similar as the mesh is refined. We also note that all contributions, and in particular the true error, are larger in magnitude for the case $Re = 2000$.

We now consider a higher order space for the velocity pair (\mathbf{u}, p) . In particular, we take $(\mathbb{P}^3, \mathbb{P}^1, \mathbb{P}^2)$ for $(\mathbf{u}, \mathbf{b}, p)$ in Table 4.11 for $Re = 1000$ and Table 4.13 for $Re = 2000$. In both cases, the error is now dominated by the contribution E_M . The case of $Re = 2000$ is particularly interesting, as the error increases as the mesh is refined from 1600 elements to 3600 elements. This seemingly anomalous behavior is explained by examining the error contributions. For $\#Elements = 1600$ we have $E_{mom} + E_{con}$ has magnitude comparable to that of E_M but opposite sign, and hence there is cancellation of error. For $\#Elements = 3600$, the magnitude of $E_{mom} + E_{con}$ is much less than that of E_M and hence the total error increases as there is less cancellation of error. Hence, adjoint based analysis not only quantifies the error, it also helps in diagnosing such anomalous behavior.

Chapter 4. Adjoint based analysis for MHD

# Elements	True Error	Eff.	E_{mom}	E_{con}	E_M
1600	-3.93e-05	0.99	-1.05e-05	-2.47e-05	-3.78e-06
3600	-9.50e-06	0.97	-2.23e-06	-5.23e-06	-1.74e-06
6400	-3.41e-06	0.98	-8.12e-07	-1.52e-06	-9.87e-07
10000	-1.61e-06	0.98	-3.64e-07	-5.81e-07	-6.33e-07

Table 4.10: Error estimates for $(b_y, \mathbb{1}_{\Omega_c})$ for the lid driven cavity §4.4.2. The finite dimensional space here is $(\mathbb{P}^2, \mathbb{P}^1, \mathbb{P}^1)$ for $(\mathbf{u}, \mathbf{b}, p)$. We use an overkill solution on a $400 \times 400 = 160000$ element mesh and $(\mathbb{P}^3, \mathbb{P}^2, \mathbb{P}^2)$ elements. The parameters are $Re = 1000, Re_m = 0.4, \kappa = 1$.

# Elements	True Error	Eff.	E_{mom}	E_{con}	E_M
1600	-5.37e-06	0.98	-4.65e-07	-9.75e-07	-3.81e-06
3600	-1.95e-06	0.99	-5.49e-08	-1.27e-07	-1.75e-06
6400	-1.03e-06	1.00	-1.06e-08	-2.76e-08	-9.87e-07
10000	-6.45e-07	1.00	-2.89e-09	-8.04e-09	-6.33e-07

Table 4.11: Error estimates for in $(b_y, \mathbb{1}_{\Omega_c})$ for the lid driven cavity §4.4.2. The finite dimensional space here is $(\mathbb{P}^3, \mathbb{P}^1, \mathbb{P}^2)$ for $(\mathbf{u}, \mathbf{b}, p)$. We use an overkill solution on a $400 \times 400 = 160000$ element mesh and $(\mathbb{P}^3, \mathbb{P}^2, \mathbb{P}^2)$ elements. The parameters are $Re = 1000, Re_m = 0.4, \kappa = 1$.

# Elements	True Error	Eff.	E_{mom}	E_{con}	E_M
1600	-8.01e-05	1.10	-3.65e-05	-5.70e-05	5.63e-06
3600	-2.04e-05	0.98	-5.69e-06	-1.66e-05	2.25e-06
6400	-5.92e-06	0.96	-1.84e-06	-5.06e-06	1.19e-06
10000	-2.07e-06	0.96	-8.17e-07	-1.91e-06	7.41e-07

Table 4.12: Error estimates for $(b_y, \mathbb{1}_{\Omega_c})$ for the lid driven cavity §4.4.2. The finite dimensional space here is $(\mathbb{P}^2, \mathbb{P}^1, \mathbb{P}^1)$ for $(\mathbf{u}, \mathbf{b}, p)$. We use an overkill solution on a $400 \times 400 = 160000$ element mesh and $(\mathbb{P}^3, \mathbb{P}^2, \mathbb{P}^2)$ elements. The parameters are $Re = 2000, Re_m = 0.4, \kappa = 1$.

# Elements	True Error	Eff.	E_{mom}	E_{con}	E_M
1600	1.31e-06	0.78	-1.58e-06	-3.47e-06	6.08e-06
3600	1.51e-06	0.96	-1.91e-07	-5.29e-07	2.17e-06
6400	1.02e-06	0.98	-3.87e-08	-1.28e-07	1.17e-06
10000	6.94e-07	0.99	-1.07e-08	-4.04e-08	7.38e-07

Table 4.13: Error estimates for $(b_y, \mathbb{1}_{\Omega_c})$ for the lid driven cavity §4.4.2. The finite dimensional space here is $(\mathbb{P}^3, \mathbb{P}^1, \mathbb{P}^2)$ for $(\mathbf{u}, \mathbf{b}, p)$. We use an overkill solution on a $400 \times 400 = 160000$ element mesh and $(\mathbb{P}^3, \mathbb{P}^2, \mathbb{P}^2)$ elements. The parameters are $\text{Re} = 2000, \text{Re}_m = 0.4, \kappa = 1$.

4.5 Well posedness and derivation of the weak adjoint problem

In this chapter we provide the details of computing the adjoint to exact penalty weak form following the theory in §4.2. Then we use a standard saddle point argument to demonstrate the well-posedness of this new adjoint problem (4.23). We take inspiration for these proofs from [39]. To simplify notation in this section, we define

$$\mathbf{s} := \mathbf{u} + \mathbf{u}_h, \quad \mathbf{t} := \mathbf{b} + \mathbf{b}_h. \quad (4.35)$$

4.5.1 Derivation of the weak form of the adjoint

In this section we provide derivation for the primal linearized operators $\overline{\mathcal{J}}_{21}^* = \overline{\mathcal{Y}}^*$, $\overline{\mathcal{J}}_{11}^* = \overline{\mathcal{Z}}_{\mathbf{u}}^*$, $\overline{\mathcal{J}}_{12}^* = \overline{\mathcal{Z}}_{\mathbf{b}}^*$ and $\overline{\mathcal{J}}_{31}^* = \mathcal{C}^*$ in (4.22). We first compute the primal linearized operators, $\overline{\mathcal{Y}} = \overline{\mathcal{J}}_{21}$, $\overline{\mathcal{Z}}_{\mathbf{u}} = \overline{\mathcal{J}}_{11}$, $\overline{\mathcal{Z}}_{\mathbf{b}} = \overline{\mathcal{J}}_{12}$ and $\mathcal{C} = \overline{\mathcal{J}}_{31}$, using (4.15) and then apply (4.16) to compute the $\overline{\mathcal{J}}_{ij}^*$ s. We have from (4.15),

$$\overline{\mathcal{Y}} \mathbf{d} := \int_0^1 \frac{\partial \mathcal{Y}}{\partial \mathbf{b}} (\mathbf{s} \mathbf{b} + (1-s) \mathbf{b}_h) \mathbf{d} \, ds, \quad (4.36a)$$

$$\overline{\mathcal{Z}}_{\mathbf{b}} \mathbf{d} := \int_0^1 \frac{\partial \mathcal{Z}}{\partial \mathbf{b}} (\mathbf{s} \mathbf{u} + (1-s) \mathbf{u}_h) \mathbf{d} \, ds, \quad (4.36b)$$

$$\overline{\mathcal{Z}}_{\mathbf{u}} \mathbf{w} := \int_0^1 \frac{\partial \mathcal{Z}}{\partial \mathbf{u}} (\mathbf{s} \mathbf{b} + (1-s) \mathbf{b}_h) \mathbf{w} \, ds. \quad (4.36c)$$

Chapter 4. Adjoint based analysis for MHD

In order to take advantage of the product rule for Banach spaces, Theorem 3.1.4. In particular, one has that

$$\nabla \times (\mathbf{v} \times \mathbf{c}) = \mathbf{v}(\nabla \cdot \mathbf{c}) - \mathbf{c}(\nabla \cdot \mathbf{v}) + (\mathbf{c} \cdot \nabla)\mathbf{v} - (\mathbf{v} \cdot \nabla)\mathbf{c}. \quad (4.37)$$

Using Corollary 1 we can take the Fréchet derivatives in (4.36b) and (4.36c),

$$\begin{aligned} \frac{\partial \mathcal{Z}}{\partial \mathbf{b}} \mathbf{c} &= \frac{\partial}{\partial \mathbf{b}} (\mathbf{u}(\nabla \cdot \mathbf{b}) - \mathbf{b}(\nabla \cdot \mathbf{u}) + (\mathbf{b} \cdot \nabla)\mathbf{u} - (\mathbf{u} \cdot \nabla)\mathbf{b})\mathbf{c} \\ &= \frac{\partial}{\partial \mathbf{b}} (\mathbf{u}(\nabla \cdot \mathbf{b}) - \mathbf{b}(\nabla \cdot \mathbf{u}) + (\nabla \mathbf{u})\mathbf{b} - (\nabla \mathbf{b})\mathbf{u})\mathbf{c} \\ &= (\mathbf{u}(\nabla \cdot \mathbf{c}) - \mathbf{c}(\nabla \cdot \mathbf{u}) + (\nabla \mathbf{u})\mathbf{c} - (\nabla \mathbf{c})\mathbf{u}) \\ &= \nabla \times (\mathbf{u} \times \mathbf{c}) \end{aligned}$$

and by symmetry of (4.37),

$$\frac{\partial \mathcal{Z}}{\partial \mathbf{u}} \mathbf{v} = \nabla \times (\mathbf{v} \times \mathbf{b}). \quad (4.38)$$

Finally, the Fréchet derivative in (4.36a) can immediately be obtained by appealing to Corollary 2.

Now we are prepared to compute for $\mathbf{d} \in \mathbf{H}_\tau^1(\Omega)$,

$$\begin{aligned} \overline{\mathcal{Y}} \mathbf{d} &= \int_0^1 \frac{\partial \mathcal{Y}}{\partial \mathbf{b}} (s\mathbf{b} + (1-s)\mathbf{b}_h) \mathbf{d} \, ds \\ &= \int_0^1 [\nabla \times (s\mathbf{b} + (1-s)\mathbf{b}_h)] \times \mathbf{d} + (\nabla \times \mathbf{d}) \times (s\mathbf{b} + (1-s)\mathbf{b}_h) \, ds \\ &= \frac{1}{2} [(\nabla \times (\mathbf{b}_h + \mathbf{b})) \times \mathbf{d} + (\nabla \times \mathbf{d}) \times (\mathbf{b}_h + \mathbf{b})]. \end{aligned} \quad (4.39)$$

Similarly, for the two $\overline{\mathcal{Z}}$ terms for $\mathbf{d} \in \mathbf{H}_\tau^1(\Omega)$,

$$\begin{aligned} \overline{\mathcal{Z}}_b \mathbf{d} &= \int_0^1 \frac{\partial \mathcal{Z}}{\partial \mathbf{b}} (s\mathbf{u} + (1-s)\mathbf{u}_h) \mathbf{d} \, ds \\ &= \int_0^1 \nabla \times ((s\mathbf{u} + (1-s)\mathbf{u}_h) \times \mathbf{d}) \, ds = \frac{1}{2} [\nabla \times ((\mathbf{u}_h + \mathbf{u}) \times \mathbf{d})]. \end{aligned} \quad (4.40)$$

An identical procedure produces,

$$\overline{\mathcal{Z}}_u \mathbf{w} = \frac{1}{2} [\nabla \times (\mathbf{w} \times (\mathbf{b} + \mathbf{b}_h))]. \quad (4.41)$$

Now, to find the adjoints of these operators, we use (4.16), which in our case involves multiplying by a test function and then isolating the trial function using integration by parts. We also make use of the vector identities in Appendix B.

We now compute the adjoint for $\overline{\mathcal{Y}}$. Integrating (4.39) against $\mathbf{v} \in \mathbf{H}_0^1(\Omega)$,

$$\begin{aligned}
 (\overline{\mathcal{Y}}\mathbf{d}, \mathbf{v}) &= \frac{1}{2} \int_{\Omega} [(\nabla \times \mathbf{t}) \times \mathbf{d} + (\nabla \times \mathbf{d}) \times \mathbf{t}] \cdot \mathbf{v} \, dx \\
 &\stackrel{(B.1)}{=} \frac{1}{2} \int_{\Omega} \mathbf{d} \cdot [\mathbf{v} \times (\nabla \times \mathbf{t})] + (\nabla \times \mathbf{d}) \cdot [\mathbf{t} \times \mathbf{v}] \, dx \\
 &\stackrel{(B.5)}{=} \frac{1}{2} \int_{\Omega} -\mathbf{d} \cdot [(\nabla \times \mathbf{t}) \times \mathbf{v}] + \mathbf{d} \cdot [\nabla \times (\mathbf{t} \times \mathbf{v})] \, dx - \frac{1}{2} \int_{\partial\Omega} \mathbf{d} \cdot [(\mathbf{t} \times \mathbf{v}) \times \mathbf{n}] \, ds \\
 &\stackrel{(B.1)}{=} \frac{1}{2} \int_{\Omega} -\mathbf{d} \cdot [(\nabla \times \mathbf{t}) \times \mathbf{v}] + \mathbf{d} \cdot [\nabla \times (\mathbf{t} \times \mathbf{v})] \, dx + \frac{1}{2} \int_{\partial\Omega} (\mathbf{t} \times \mathbf{v}) \cdot [\mathbf{d} \times \mathbf{n}] \, ds \\
 &\stackrel{(4.4)}{=} \frac{1}{2} \int_{\Omega} -\mathbf{d} \cdot [(\nabla \times \mathbf{t}) \times \mathbf{v}] + \mathbf{d} \cdot [\nabla \times (\mathbf{t} \times \mathbf{v})] \, dx \stackrel{(4.22)}{=} (\mathbf{d}, \overline{\mathcal{Y}}^* \mathbf{v}).
 \end{aligned}$$

We proceed with computing the adjoint for $\overline{\mathcal{Z}}_u$, by integrating against $\mathbf{c} \in \mathbf{H}_{\tau}^1(\Omega)$,

$$\begin{aligned}
 (\overline{\mathcal{Z}}_u \mathbf{w}, \mathbf{c}) &= \frac{1}{2} \int_{\Omega} \nabla \times (\mathbf{w} \times \mathbf{t}) \cdot \mathbf{c} \, dx \\
 &\stackrel{(B.5)}{=} \frac{1}{2} \int_{\Omega} (\mathbf{w} \times \mathbf{t}) \cdot (\nabla \times \mathbf{c}) \, dx - \frac{1}{2} \int_{\partial\Omega} (\mathbf{w} \times \mathbf{t}) \cdot (\mathbf{c} \times \mathbf{n}) \, ds \\
 &\stackrel{(B.1)}{=} \frac{1}{2} \int_{\Omega} \mathbf{w} \cdot [\mathbf{t} \times (\nabla \times \mathbf{c})] \, dx - \frac{1}{2} \int_{\partial\Omega} (\mathbf{w} \times \mathbf{t}) \cdot (\mathbf{c} \times \mathbf{n}) \, ds \\
 &\stackrel{(4.3)}{=} \frac{1}{2} \int_{\Omega} \mathbf{w} \cdot [\mathbf{t} \times (\nabla \times \mathbf{c})] \, dx \stackrel{(4.22)}{=} (\mathbf{w}, \overline{\mathcal{Z}}_u^* \mathbf{c}).
 \end{aligned}$$

Finally we compute the adjoint to the linearized operator $\overline{\mathcal{Z}}_b$ by integrating against $\mathbf{c} \in \mathbf{H}_{\tau}^1(\Omega)$,

$$\begin{aligned}
 (\overline{\mathcal{Z}}_b \mathbf{d}, \mathbf{c}) &= \frac{1}{2} (\nabla \times (\mathbf{s} \times \mathbf{d}), \mathbf{c}) \\
 &\stackrel{(B.5)}{=} \frac{1}{2} \int_{\Omega} (\mathbf{s} \times \mathbf{d}) \cdot (\nabla \times \mathbf{c}) \, dx - \frac{1}{2} \int_{\partial\Omega} (\mathbf{s} \times \mathbf{d}) \cdot (\mathbf{c} \times \mathbf{n}) \, ds \\
 &\stackrel{(B.1)}{=} \frac{1}{2} \int_{\Omega} \mathbf{d} \cdot [(\nabla \times \mathbf{c}) \times \mathbf{s}] \, dx - \frac{1}{2} \int_{\partial\Omega} \mathbf{d} \cdot [\mathbf{s} \times (\mathbf{c} \times \mathbf{n})] - (\mathbf{s} \times \mathbf{d}) \cdot (\mathbf{c} \times \mathbf{n}) \, ds \\
 &\stackrel{(4.4)}{=} \frac{1}{2} \int_{\Omega} \mathbf{d} \cdot [(\nabla \times \mathbf{c}) \times \mathbf{s}] \, dx \stackrel{(4.22)}{=} (\mathbf{d}, \overline{\mathcal{Z}}_b^* \mathbf{c}).
 \end{aligned}$$

The operator \mathcal{C}^* is identical to the one presented in [33], and the derivation can be seen in §3.4.

4.5.2 Well posedness of the adjoint problem

In this section we prove the well-posedness of the adjoint problem §4.3.1 equation (4.23) using a saddle point type argument. To keep consistent with the standard setting of saddle point problems [26, 13], we use the notation $X := \mathbf{H}_0^1(\Omega) \times \mathbf{H}_\tau^1(\Omega)$ and $M := L^2(\Omega)$ so that $\mathcal{P}(\Omega) = X \times M$. We equip the space X with the graph norm

$$\|(\mathbf{v}, \mathbf{c})\|_X := (\|\mathbf{v}\|_1^2 + \|\mathbf{c}\|_1^2)^{1/2}. \quad (4.42)$$

We next define the bilinear form $a : X \rightarrow \mathbb{R}$ by

$$\begin{aligned} a((\phi, \boldsymbol{\beta}), (\mathbf{v}, \mathbf{c})) &= \frac{1}{\text{Re}} (\nabla \phi, \nabla \mathbf{v}) + (\overline{\mathbf{c}}^* \phi, \mathbf{v}) \\ &+ \frac{\kappa}{\text{Re}_m} (\nabla \times \boldsymbol{\beta}, \nabla \times \mathbf{c}) + \frac{\kappa}{\text{Re}_m} (\nabla \cdot \boldsymbol{\beta}, \nabla \cdot \mathbf{c}) \\ &- \kappa (\overline{\mathbf{y}}^* \phi, \mathbf{c}) - \kappa (\overline{\mathbf{z}}_u^* \boldsymbol{\beta}, \mathbf{v}) - \kappa (\overline{\mathbf{z}}_b^* \boldsymbol{\beta}, \mathbf{c}), \end{aligned} \quad (4.43)$$

and the mixed form $b : X \times M \rightarrow \mathbb{R}$ by

$$b((\mathbf{v}, \mathbf{c}), \pi) = -(\pi, \nabla \cdot \mathbf{v}). \quad (4.44)$$

The weak dual problem (4.23) is then equivalent to the following mixed problem: find $((\phi, \boldsymbol{\beta}), \pi) \in X \times M$ such that

$$\begin{cases} a((\phi, \boldsymbol{\beta}), (\mathbf{v}, \mathbf{c})) + b((\mathbf{v}, \mathbf{c}), p) = (\psi, \mathbf{v}), & \forall (\mathbf{v}, \mathbf{c}) \in X, \\ b((\phi, \boldsymbol{\beta}), q) = (\psi_p, q), & \forall q \in M. \end{cases} \quad (4.45)$$

According the theory of saddle point systems, in order to show the existence and uniqueness of solutions to (4.45), it suffices to show three things:

- (i) The bilinear forms $a(\cdot, \cdot)$ and $b(\cdot, \cdot)$ are bounded on their respective domains.
- (ii) The form $a(\cdot, \cdot)$ is coercive on $X_0 := \{v \in X : b(v, q) = 0, \forall q \in M\}$.

(iii) The form $b(\cdot, \cdot)$ satisfies the inf-sup condition: $\exists \beta > 0$ such that

$$\inf_{q \in M} \sup_{(\mathbf{v}, \mathbf{c}) \in X} \frac{b((\mathbf{v}, \mathbf{c}), q)}{\|(\mathbf{v}, \mathbf{c})\|_X \|q\|_M} \geq \beta. \quad (4.46)$$

We organize these parts in the following lemmas. We make frequent use of the inequalities in C in the proofs.

Lemma 4.5.1. *The form $a(\cdot, \cdot)$ is bounded on X .*

Proof. Consider the splitting

$$a((\phi, \beta), (\mathbf{v}, \mathbf{c})) = a_0((\phi, \beta), (\mathbf{v}, \mathbf{c})) + a_1((\phi, \beta), (\mathbf{v}, \mathbf{c})) \quad (4.47)$$

where

$$\begin{aligned} a_0((\phi, \beta), (\mathbf{v}, \mathbf{c})) &= \frac{1}{\text{Re}} (\nabla \phi, \nabla \mathbf{v}) + \frac{\kappa}{\text{Re}_m} (\nabla \times \beta, \nabla \times \mathbf{c}) + \frac{\kappa}{\text{Re}_m} (\nabla \cdot \beta, \nabla \cdot \mathbf{c}), \\ a_1((\phi, \beta), (\mathbf{v}, \mathbf{c})) &= (\bar{\mathcal{C}}^* \phi, \mathbf{v}) - \kappa (\bar{\mathcal{Y}}^* \phi, \mathbf{c}) - \kappa (\bar{\mathcal{Z}}_u^* \beta, \mathbf{v}) - \kappa (\bar{\mathcal{Z}}_b^* \beta, \mathbf{c}). \end{aligned}$$

Then it suffices to show that both a_0 and a_1 are bounded separately. The proof for the boundedness of a_0 is given in [39]. For a_1 observe that

$$\begin{aligned} |a_1((\phi, \beta), (\mathbf{v}, \mathbf{c}))| &\leq \int_{\Omega} |\bar{\mathcal{C}}^* \phi \cdot \mathbf{v}| \, dx + \kappa \int_{\Omega} |\bar{\mathcal{Y}}^* \phi \cdot \mathbf{c}| \, dx \\ &\quad + \kappa \int_{\Omega} |\bar{\mathcal{Z}}_u^* \beta \cdot \mathbf{v}| \, dx + \kappa \int_{\Omega} |\bar{\mathcal{Z}}_b^* \beta \cdot \mathbf{c}| \, dx. \end{aligned} \quad (4.48)$$

Now, for the first term on the right hand side of (4.48),

$$\begin{aligned} \int_{\Omega} |\bar{\mathcal{C}}^* \phi \cdot \mathbf{v}| \, dx &= \frac{1}{2} \int_{\Omega} |[(\nabla \mathbf{s})^T \phi - ((\mathbf{s} \cdot \nabla) \phi) - (\nabla \cdot \mathbf{s}) \phi] \cdot \mathbf{v}| \, dx \\ &= \frac{1}{2} \int_{\Omega} |\phi^T (\nabla \mathbf{s}) \mathbf{v} - \mathbf{v}^T (\nabla \phi) \mathbf{s} - (\nabla \cdot \mathbf{s}) (\phi \cdot \mathbf{v})| \, dx \\ &\stackrel{\text{(C.7)}}{\leq} \frac{1}{2} [\|\phi\|_{L^4} \|\mathbf{s}\|_1 \|\mathbf{v}\|_{L^4} + \|\phi\|_1 \|\mathbf{s}\|_{L^4} \|\mathbf{v}\|_{L^4} + \|\nabla \cdot \mathbf{s}\| \|\phi \cdot \mathbf{v}\|] \\ &\stackrel{\text{(B.8d)}}{\leq} \frac{1}{2} [\|\phi\|_{L^4} \|\mathbf{s}\|_1 \|\mathbf{v}\|_{L^4} + \|\phi\|_1 \|\mathbf{s}\|_{L^4} \|\mathbf{v}\|_{L^4} + \sqrt{3} \|\mathbf{s}\|_1 \|\phi\|_{L^4} \|\mathbf{v}\|_{L^4}] \\ &\stackrel{\text{(C.1)}}{\leq} \frac{\gamma}{2} (\|\phi\|_1 \|\mathbf{s}\|_1 \|\mathbf{v}\|_1 + \|\mathbf{s}\|_1 \|\phi\|_1 \|\mathbf{v}\|_1 + \sqrt{3} \|\mathbf{s}\|_1 \|\phi\|_1 \|\mathbf{v}\|_1) \\ &\leq \frac{3\sqrt{3}\gamma}{2} \|\mathbf{s}\|_1 \|\phi\|_1 \|\mathbf{v}\|_1, \end{aligned}$$

Chapter 4. Adjoint based analysis for MHD

where γ is the square of the embedding constant of $\mathbf{H}^1(\Omega)$ into $\mathbf{L}^4(\Omega)$, see (C.1).

For the second term on the right hand side of (4.48),

$$\begin{aligned}
\kappa \left(\overline{\mathcal{Y}}^* \phi \cdot \mathbf{c} \right) &\leq \frac{\kappa}{2} \int_{\Omega} \left| \mathbf{c} \cdot [(\nabla \times \mathbf{t}) \times \phi] \right| + \left| \mathbf{c} \cdot [\nabla \times (\mathbf{t} \times \phi)] \right| dx \\
&\stackrel{\text{(B.5)}}{=} \frac{\kappa}{2} \int_{\Omega} \left| \mathbf{c} \cdot ((\nabla \times \mathbf{t}) \times \phi) \right| + \left| (\nabla \times \mathbf{c}) \cdot (\mathbf{t} \times \phi) \right| dx \\
&\stackrel{\text{(B.1)}}{=} \frac{\kappa}{2} \int_{\Omega} \left| (\nabla \times \mathbf{t}) \cdot (\mathbf{c} \times \phi) \right| + \left| (\nabla \times \mathbf{c}) \cdot (\mathbf{t} \times \phi) \right| dx \\
&\stackrel{\text{(B.8b)}}{\leq} \frac{\kappa}{2} \left(\|\nabla \times \mathbf{t}\|_{L^2} \|\mathbf{c}\|_{L^4} \|\phi\|_{L^4} + \|\nabla \times \mathbf{c}\|_{L^2} \|\mathbf{t}\|_{L^4} \|\phi\|_{L^4} \right) \\
&\stackrel{\text{(B.8c)}}{\leq} \frac{\kappa\sqrt{2}}{2} \left(\|\mathbf{c}\|_{L^4} \|\mathbf{t}\|_1 \|\phi\|_{L^4} + \|\mathbf{c}\|_1 \|\mathbf{t}\|_{L^4} \|\phi\|_{L^4} \right) \\
&\stackrel{\text{(C.1)}}{\leq} \kappa\gamma\sqrt{2} \|\mathbf{c}\|_1 \|\mathbf{t}\|_1 \|\phi\|_1.
\end{aligned}$$

For the third term on the right hand side of (4.48),

$$\begin{aligned}
\kappa \left(\overline{\mathcal{Z}}_u^* \boldsymbol{\beta}, \mathbf{v} \right) &\leq \frac{\kappa}{2} \int_{\Omega} \left| \mathbf{v} \cdot [\mathbf{t} \times (\nabla \times \boldsymbol{\beta})] \right| dx \stackrel{\text{(B.5)}}{=} \frac{\kappa}{2} \int_{\Omega} \left| (\mathbf{v} \times \mathbf{t}) \cdot (\nabla \times \boldsymbol{\beta}) \right| dx \\
&\stackrel{\text{(B.8c)}}{\leq} \frac{\kappa\sqrt{2}}{2} \|\mathbf{v}\|_{L^4} \|\mathbf{t}\|_{L^4} \|\boldsymbol{\beta}\|_1 \stackrel{\text{(C.1)}}{\leq} \frac{\kappa\gamma\sqrt{2}}{2} \|\mathbf{v}\|_1 \|\mathbf{t}\|_1 \|\boldsymbol{\beta}\|_1.
\end{aligned}$$

The fourth term follows the same argument as the third term to yield the bound,

$$\kappa \left(\overline{\mathcal{Z}}_b^* \boldsymbol{\beta}, \mathbf{c} \right) \leq \frac{\kappa\gamma\sqrt{2}}{2} \|\mathbf{c}\|_1 \|\mathbf{s}\|_1 \|\boldsymbol{\beta}\|_1. \tag{4.49}$$

Putting these bounds together, we conclude

$$\begin{aligned}
 a_1((\boldsymbol{\phi}, \boldsymbol{\beta}), (\mathbf{v}, \mathbf{c})) &\leq \gamma \left(\frac{3\sqrt{3}}{2} \|\mathbf{s}\|_1 \|\boldsymbol{\phi}\|_1 \|\mathbf{v}\|_1 + \kappa\sqrt{2} \|\mathbf{c}\|_1 \|\mathbf{t}\|_1 \|\boldsymbol{\phi}\|_1 \right. \\
 &\quad \left. + \frac{\kappa\sqrt{2}}{2} \|\mathbf{v}\|_1 \|\mathbf{t}\|_1 \|\boldsymbol{\beta}\|_1 + \frac{\kappa\sqrt{2}}{2} \|\mathbf{c}\|_1 \|\mathbf{s}\|_1 \|\boldsymbol{\beta}\|_1 \right) \\
 &\stackrel{(C.4)}{\leq} \gamma \left(\frac{3\sqrt{3}}{2} \|\mathbf{s}\|_1 \|\boldsymbol{\phi}\|_1 \|\mathbf{v}\|_1 + \frac{\kappa\sqrt{2}}{2} \|\mathbf{c}\|_1 \|\mathbf{s}\|_1 \|\boldsymbol{\beta}\|_1 \right. \\
 &\quad \left. + \|\mathbf{t}\|_1 \kappa\sqrt{2} \|(\mathbf{v}, \mathbf{c})\|_X \|(\boldsymbol{\phi}, \boldsymbol{\beta})\|_X \right) \tag{4.50} \\
 &\stackrel{(C.4)}{\leq} \gamma \left(\|\mathbf{s}\|_1 \max \left\{ \frac{3\sqrt{3}}{2}, \frac{\kappa\sqrt{2}}{2} \right\} \|(\mathbf{v}, \mathbf{c})\|_X \|(\boldsymbol{\phi}, \boldsymbol{\beta})\|_X \right. \\
 &\quad \left. + \|\mathbf{t}\|_1 \|(\mathbf{v}, \mathbf{c})\|_X \|(\boldsymbol{\phi}, \boldsymbol{\beta})\|_X \right) \\
 &\leq \alpha_b \|(\mathbf{v}, \mathbf{c})\|_X \|(\boldsymbol{\phi}, \boldsymbol{\beta})\|_X,
 \end{aligned}$$

where in turn

$$\alpha_b = \max \left\{ \|\mathbf{s}\|_1 \max \left\{ \frac{3\sqrt{3}}{2}, \frac{\kappa\sqrt{2}}{2} \right\}, \|\mathbf{t}\|_1 \right\}.$$

□

Now we consider the coercivity of the bilinear form $a(\cdot, \cdot)$ on X .

Lemma 4.5.2. *There exists a constant $\alpha_c > 0$ such that whenever*

$$\frac{k_1}{Re} - \gamma \left[\frac{3\sqrt{3}}{2} \|\mathbf{s}\|_1 + \frac{3\kappa\sqrt{2}}{4} \|\mathbf{t}\|_1 \right] > 0, \tag{4.51}$$

and

$$\frac{k_2\kappa}{Re_m^2} - \gamma \left[\frac{\kappa\sqrt{2}}{2} \|\mathbf{s}\|_1 + \frac{3\kappa\sqrt{2}}{4} \|\mathbf{t}\|_1 \right] > 0 \tag{4.52}$$

then

$$a((\boldsymbol{\phi}, \boldsymbol{\beta}), (\boldsymbol{\phi}, \boldsymbol{\beta})) \geq \alpha_c \|(\boldsymbol{\phi}, \boldsymbol{\beta})\|_X^2, \quad \forall (\boldsymbol{\phi}, \boldsymbol{\beta}) \in X. \tag{4.53}$$

Proof. Using the splitting established in the previous lemma,

$$\begin{aligned}
a((\boldsymbol{\phi}, \boldsymbol{\beta}), (\boldsymbol{\phi}, \boldsymbol{\beta})) &\geq a_0((\boldsymbol{\phi}, \boldsymbol{\beta}), (\boldsymbol{\phi}, \boldsymbol{\beta})) - |a_1((\boldsymbol{\phi}, \boldsymbol{\beta}), (\boldsymbol{\phi}, \boldsymbol{\beta}))| \\
&= \frac{1}{\text{Re}} (\nabla \boldsymbol{\phi}, \nabla \boldsymbol{\phi}) + \frac{\kappa}{\text{Re}_m} (\nabla \times \boldsymbol{\beta}, \nabla \times \boldsymbol{\beta}) + \frac{\kappa}{\text{Re}_m} (\nabla \cdot \boldsymbol{\beta}, \nabla \cdot \boldsymbol{\beta}) \\
&\quad - |a_1((\boldsymbol{\phi}, \boldsymbol{\beta}), (\boldsymbol{\phi}, \boldsymbol{\beta}))| \\
&\geq \frac{k_1}{\text{Re}} \|\boldsymbol{\phi}\|_1^2 + \frac{k_2 \kappa}{\text{Re}_m^2} \|\boldsymbol{\beta}\|_1^2 - |a_1((\boldsymbol{\phi}, \boldsymbol{\beta}), (\boldsymbol{\phi}, \boldsymbol{\beta}))|
\end{aligned} \tag{4.54}$$

where k_1 comes from the Poincaré inequality (C.5), and k_2 is defined though

$$\|\nabla \times \boldsymbol{v}\|_0^2 + \|\nabla \cdot \boldsymbol{v}\|_0^2 \geq k_2 \|\boldsymbol{v}\|_1^2, \quad \forall \boldsymbol{v} \in \mathbf{H}_\tau^1(\Omega), \tag{4.55}$$

which is valid under the restrictions we have imposed on the domain Ω and the continuous embedding of $\mathbf{H}_\tau^1(\Omega) \hookrightarrow \mathbf{H}^1(\Omega)$ [37]. Picking up from (4.54) and using (C.6) we conclude that,

$$\begin{aligned}
a((\boldsymbol{\phi}, \boldsymbol{\beta}), (\boldsymbol{\phi}, \boldsymbol{\beta})) &\geq \frac{k_1}{\text{Re}} \|\boldsymbol{\phi}\|_1^2 + \frac{k_2 \kappa}{\text{Re}_m^2} \|\boldsymbol{\beta}\|_1^2 - |a_1((\boldsymbol{\phi}, \boldsymbol{\beta}), (\boldsymbol{\phi}, \boldsymbol{\beta}))| \\
&\stackrel{(4.50)}{\geq} \left(\frac{k_1}{\text{Re}} - \frac{\gamma 3\sqrt{3}}{2} \|\mathbf{s}\|_1 \right) \|\boldsymbol{\phi}\|_1^2 + \left(\frac{k_2 \kappa}{\text{Re}_m^2} - \frac{\gamma \kappa \sqrt{2}}{2} \|\mathbf{s}\|_1 \right) \|\boldsymbol{\beta}\|_1^2 \\
&\quad - \frac{\gamma 3\kappa \sqrt{2}}{2} \|\boldsymbol{\phi}\|_1 \|\boldsymbol{\beta}\|_1 \\
&\stackrel{(C.6)}{\geq} \left(\frac{k_1}{\text{Re}} - \frac{\gamma 3\sqrt{3}}{2} \|\mathbf{s}\|_1 \right) \|\boldsymbol{\phi}\|_1^2 + \left(\frac{k_2 \kappa}{\text{Re}_m^2} - \frac{\gamma \kappa \sqrt{2}}{2} \|\mathbf{s}\|_1 \right) \|\boldsymbol{\beta}\|_1^2 \\
&\quad - \frac{\gamma 3\kappa \sqrt{2}}{4} \|\boldsymbol{t}\|_1 (\|\boldsymbol{\beta}\|_1^2 + \|\boldsymbol{\phi}\|_1^2) \\
&= \left(\frac{k_1}{\text{Re}} - \gamma \left[\frac{3\sqrt{3}}{2} \|\mathbf{s}\|_1 + \frac{3\kappa \sqrt{2}}{4} \|\boldsymbol{t}\|_1 \right] \right) \|\boldsymbol{\phi}\|_1^2 \\
&\quad + \left(\frac{k_2 \kappa}{\text{Re}_m^2} - \gamma \left[\frac{\kappa \sqrt{2}}{2} \|\mathbf{s}\|_1 + \frac{3\kappa \sqrt{2}}{4} \|\boldsymbol{t}\|_1 \right] \right) \|\boldsymbol{\beta}\|_1^2.
\end{aligned}$$

Thus, taking

$$\begin{aligned}
\alpha_c = \min \left\{ \frac{k_1}{\text{Re}} - \gamma \left[\frac{3\sqrt{3}}{2} \|\mathbf{s}\|_1 + \frac{3\kappa \sqrt{2}}{4} \|\boldsymbol{t}\|_1 \right], \right. \\
\left. \frac{k_2 \kappa}{\text{Re}_m^2} - \gamma \left[\frac{\kappa \sqrt{2}}{2} \|\mathbf{s}\|_1 + \frac{3\kappa \sqrt{2}}{4} \|\boldsymbol{t}\|_1 \right] \right\},
\end{aligned} \tag{4.56}$$

concludes the lemma. □

Remark 4.5.1. *We note here the quantities we had to assume were positive (4.51) and (4.52), depend on the computed and true solutions through $\|\mathbf{s}\|, \|\mathbf{t}\|$, which should both be bounded for a stable solution. The two quantities (4.51) and (4.52) also depend on the fluid and magnetic Reynolds numbers (respectively Re and Re_m). In particular, for small to moderate Re and Re_m these inequalities might very well be satisfied. However, the larger are Re and Re_m (and in particular for the limit as $Re, Re_m \rightarrow \infty$, that is in the case of ideal MHD), the smaller the positive terms of (4.51) and (4.52), and thus coercivity cannot be proven by this method. We conclude this method might therefore need to be adapted for high Re or Re_m flows to guarantee coercivity.*

Now we are prepared to prove the main result.

Theorem 4.5.1. *Under the conditions of Lemma 4.5.2 there exists a unique solution to the dual problem (4.23).*

Proof. The boundedness and inf-sup condition for $b(\cdot, \cdot)$ are standard see e.g. [13]. The boundedness of $a(\cdot, \cdot)$ follows from Lemma 4.5.1, and Lemma 4.5.2 proves $a(\cdot, \cdot)$ is coercive on X so in particular on X_0 . □

Chapter 5

Conclusions and future directions

In this thesis, we have presented the abstract tenants of adjoint based *a posteriori* error analysis (ABAPEA) for both linear and nonlinear problems. Additionally, in chapters 2 and 3 we present concrete examples of ABAPEA for both linear and nonlinear problems. In Chapter 4, we present ABAPEA for the equations of stationary magnetohydrodynamics (MHD). This work contains several novel aspects. Firstly, since the MHD equations are over-determined, we must define an adjoint to a rectangular system. This is achieved by defining the adjoint directly to a consistent weak form, namely the exact penalty weak form. Secondly, we establish the well-posedness of the adjoint problem using techniques of saddle point theory. Thirdly, we use our MHD adjoint problem to not only provide error estimates for realistic MHD problems, we are able to distinguish components of error. We use this error decomposition to explain seemingly counterintuitive results when refining in both mesh size h and polynomial order p .

This work could be extended in several ways. One way would be to (reusing much of the analysis here) perform ABAPEA for other stabilizations of MHD. These would include compatible discretizations as well as divergence cleaning. In this context, one

Chapter 5. Conclusions and future directions

could also study divergence errors, and evaluate the different techniques. Another possible extension could be to use the error contributions (potentially computed on a coarse mesh) provided by ABAPFA to inform discretization choices for an iterative splitting algorithm that would take place on a finer mesh.

Bibliography

- [1] J. H. Adler et al. “First-Order System Least Squares for Incompressible Resistive Magnetohydrodynamics”. In: *SIAM Journal on Scientific Computing* 32.1 (Jan. 2010), pp. 229–248.
- [2] J. H. Adler et al. “Island Coalescence Using Parallel First-Order System Least Squares on Incompressible Resistive Magnetohydrodynamics”. In: *SIAM Journal on Scientific Computing* 35.5 (Jan. 2013), S171–S191.
- [3] J. H. Adler et al. “Nested Iteration and First-Order System Least Squares for Incompressible, Resistive Magnetohydrodynamics”. In: *SIAM Journal on Scientific Computing* 32.3 (Jan. 2010), pp. 1506–1526.
- [4] James H. Adler et al. “Vector-potential finite-element formulations for two-dimensional resistive magnetohydrodynamics”. In: *Computers & Mathematics with Applications* 77.2 (Jan. 2019), pp. 476–493.
- [5] M. Ainsworth and T. Oden. *A posteriori error estimation in finite element analysis*. John Wiley-Teubner, 2000.
- [6] Martin S. Alnæs et al. “The FEniCS Project Version 1.5”. In: *Archive of Numerical Software* 3.100 (2015).
- [7] Antonio Ambrosetti and Giovanni Prodi. *A primer of nonlinear analysis*. Cambridge Univ. Press, 2010.

BIBLIOGRAPHY

- [8] W. Bangerth and R. Rannacher. *Adaptive Finite Element Methods for Differential Equations*. Birkhauser Verlag, 2003.
- [9] T. J. Barth. A posteriori *Error Estimation and Mesh Adaptivity for Finite Volume and Finite Element Methods*. Vol. 41. Lecture Notes in Computational Science and Engineering. New York: Springer, 2004.
- [10] Roland Becker and Rolf Rannacher. *An optimal control approach to a posteriori error estimation in finite element methods: Acta Numerica*. Jan. 2003.
- [11] P Bochev and A Robinson. “Matching algorithms with physics: exact sequences of finite element spaces”. In: *Collected Lectures on the Preservation of Stability Under Discretization, edited by D. Estep and S. Tavener, SIAM, Philadelphia (2001)*.
- [12] Daniele Boffi, Franco Brezzi, Michel Fortin, et al. *Mixed finite element methods and applications*. Vol. 44. Springer, 2013.
- [13] Susanne C. Brenner and L. Ridgway. Scott. *The mathematical theory of finite element methods*. Springer, 2011.
- [14] V. Carey, D. Estep, and S.J. Tavener. “A posteriori analysis and adaptive error control for multiscale operator decomposition solution of elliptic systems I: One way coupled systems”. In: *SIAM Journal on Numerical Analysis* 47.1 (2009), pp. 740–761.
- [15] Jehanzeb H. Chaudhry. “A Posteriori Analysis and Efficient Refinement Strategies for the Poisson–Boltzmann Equation”. In: *SIAM Journal on Scientific Computing* 40.4 (2018), A2519–A2542.
- [16] Jehanzeb H. Chaudhry, J.B. Collins, and John N. Shadid. “A posteriori error estimation for multi-stage Runge–Kutta IMEX schemes”. In: *Applied Numerical Mathematics* 117 (July 2017), pp. 36–49.

BIBLIOGRAPHY

- [17] Jehanzeb H. Chaudhry, John N. Shadid, and Timothy Wildey. “A posteriori analysis of an IMEX entropy-viscosity formulation for hyperbolic conservation laws with dissipation”. In: *Applied Numerical Mathematics* 135 (Jan. 2019), pp. 129–142.
- [18] Jehanzeb H Chaudhry, Nathaniel Burch, and Donald Estep. “Efficient Distribution Estimation and Uncertainty Quantification for Elliptic Problems on Domains with Stochastic Boundaries”. In: *SIAM/ASA Journal on Uncertainty Quantification* 6.3 (2018), pp. 1127–1150.
- [19] Jehanzeb Hameed Chaudhry et al. “A Posteriori Error Analysis of Two-Stage Computation Methods with Application to Efficient Discretization and the Parareal Algorithm”. In: *SIAM Journal on Numerical Analysis* 54.5 (2016), pp. 2974–3002.
- [20] Jehanzeb H Chaudhry et al. “A posteriori error analysis of IMEX multi-step time integration methods for advection–diffusion–reaction equations”. In: *Computer Methods in Applied Mechanics and Engineering* 285 (2015), pp. 730–751.
- [21] Jeffrey M Connors et al. “Quantification of errors for operator-split advection–diffusion calculations”. In: *Computer Methods in Applied Mechanics and Engineering* 272 (2014), pp. 181–197.
- [22] A. Dedner et al. “Hyperbolic Divergence Cleaning for the MHD Equations”. In: *Journal of Computational Physics* 175.2 (2002), pp. 645–673.
- [23] Jean Donea and Antonio Huerta. *Finite element methods for flow problems*. Wiley, 2005.
- [24] K. Eriksson et al. *Computational Differential Equations*. Cambridge: Cambridge University Press, 1996, pp. xvi+538. ISBN: 0-521-56312-7; 0-521-56738-6.
- [25] Kenneth Eriksson et al. “Introduction to Adaptive Methods for Differential Equations”. In: *Acta Numerica* 4 (Jan. 1995), pp. 105–158.

BIBLIOGRAPHY

- [26] Alexandre Ern and Jean-Luc Guermond. *Theory and practice of finite elements*. Springer, 2011.
- [27] D. J. Estep et al. *Estimating the error of numerical solutions of systems of reaction-diffusion equations*. American Mathematical Society, 2000.
- [28] D. Estep, A. Målqvist, and S. Tavener. “Nonparametric Density Estimation for Randomly Perturbed Elliptic Problems I: Computational Methods, a posteriori Analysis, and Adaptive Error Control”. In: *SIAM Journal on Scientific Computing* 31.4 (2009), pp. 2935–2959.
- [29] D. Estep, A. Målqvist, and S. Tavener. “Nonparametric density estimation for randomly perturbed elliptic problems I: Computational methods, a posteriori analysis, and adaptive error control”. In: *SIAM J. Sci. Comput.* 31 (2009), pp. 2935–2959.
- [30] D. Estep, A. Målqvist, and S. Tavener. “Nonparametric density estimation for randomly perturbed elliptic problems II: Applications and adaptive modeling”. In: *International Journal for Numerical Methods in Engineering* 80.6-7 (2009).
- [31] D. Estep et al. “An A Posteriori–A Priori Analysis of Multiscale Operator Splitting”. In: *SIAM Journal on Numerical Analysis* 46.3 (Jan. 2008), pp. 1116–1146.
- [32] Donald Estep. “A Posteriori Error Bounds and Global Error Control for Approximation of Ordinary Differential Equations”. In: *SIAM Journal on Numerical Analysis* 32.1 (Feb. 1995), pp. 1–48.
- [33] Donald Estep, Simon Tavener, and Tim Wildey. “A posteriori error estimation and adaptive mesh refinement for a multiscale operator decomposition approach to fluid-solid heat transfer”. In: *Journal of Computational Physics* 229.11 (June 2010), pp. 4143–4158.

BIBLIOGRAPHY

- [34] Charles R. Evans and John F. Hawley. “Simulation of Magnetohydrodynamic Flows: A Constrained Transport Model”. In: *Astrophysical Journal* 332 (Sept. 1988), p. 659.
- [35] J.-F. Gerbeau. “A stabilized finite element method for the incompressible magnetohydrodynamic equations”. In: *Numerische Mathematik* 87.1 (2000), pp. 83–111.
- [36] Michael B. Giles and Endre Süli. “Adjoint methods for PDEs: a posteriori error analysis and postprocessing by duality”. In: *Acta Numerica 2002* (2002), pp. 145–236.
- [37] Vivette Girault and Pierre-Arnaud Raviart. *Finite Element Methods for Navier-Stokes Equations*. Springer Berlin Heidelberg, 1986.
- [38] J. P. Hans Goedbloed et al. *Principles of Magnetohydrodynamics: With Applications to Laboratory and Astrophysical Plasmas*. Cambridge University Press, 2003.
- [39] Max D. Gunzburger, Amnon J. Meir, and Janet S. Peterson. “On the existence, uniqueness, and finite element approximation of solutions of the equations of stationary, incompressible magnetohydrodynamics”. In: *Mathematics of Computation* 56.194 (1991), pp. 523–523.
- [40] Makram Hamouda, Roger Temam, and Lee Zhang. “Modeling the lid driven flow: Theory and computation”. In: *International Journal of Numerical Analysis and Modeling* 14 (2017), pp. 313–341.
- [41] Po-Wen Hsieh and Suh-Yuh Yang. “A bubble-stabilized least-squares finite element method for steady MHD duct flow problems at high Hartmann numbers”. In: *Journal of Computational Physics* 228.22 (Dec. 2009), pp. 8301–8320.
- [42] James M. Hyman and Mikhail Shashkov. “Adjoint operators for the natural discretizations of the divergence, gradient and curl on logically rectangular grids”. In: *Applied Numerical Mathematics* 25.4 (Dec. 1997), pp. 413–442.

BIBLIOGRAPHY

- [43] Dmitri Kuzmin and Nikita Klyushnev. “Limiting and divergence cleaning for continuous finite element discretizations of the MHD equations”. In: *Journal of Computational Physics* 407 (Apr. 2020), p. 109230.
- [44] Michael W. Lee, Earl H. Dowell, and Maciej J. Balajewicz. *A study of the regularized lid-driven cavity’s progression to chaos*. Nov. 2018.
- [45] P.T. Lin et al. “Performance of fully-coupled algebraic multigrid preconditioners for large-scale VMS resistive MHD”. In: *Journal of Computational and Applied Mathematics* 344 (Dec. 2018), pp. 782–793.
- [46] Paul T. Lin, John N. Shadid, and Paul H. Tsuji. “On the performance of Krylov smoothing for fully coupled AMG preconditioners for VMS resistive MHD”. In: *International Journal for Numerical Methods in Engineering* 120.12 (Sept. 2019), pp. 1297–1309.
- [47] Anders Logg, Kent-Andre Mardal, Garth N. Wells, et al. *Automated Solution of Differential Equations by the Finite Element Method*. Springer, 2012. ISBN: 978-3-642-23098-1.
- [48] Anders Logg, Garth N. Wells, and Johan Hake. *DOLFIN: a C++/Python Finite Element Library*. Springer, 2012. Chap. 10.
- [49] Guri I. Marchuk. *Adjoint Equations and Analysis of Complex Systems*. Springer Nature, 1995. ISBN: <http://id.crossref.org/isbn/978-94-017-0621-6>.
- [50] Guri I Marchuk, Valeri I Agoshkov, and Victor P Shutyaev. *Adjoint equations and perturbation algorithms in nonlinear problems*. CRC Press, 1996.
- [51] Martin and Monique Dauge. *Weighted regularization of Maxwell equations in polyhedral domains*. Dec. 2002.
- [52] S.T. Miller et al. “IMEX and exact sequence discretization of the multi-fluid plasma model”. In: *Journal of Computational Physics* 397 (Nov. 2019), p. 108806.

BIBLIOGRAPHY

- [53] J. C. Nedelec. “Mixed finite elements in \mathbb{R}^3 ”. In: *Numerische Mathematik* 35.3 (1980), pp. 315–341.
- [54] Edward G. Phillips et al. “A Block Preconditioner for an Exact Penalty Formulation for Stationary MHD”. In: *SIAM Journal on Scientific Computing* 36.6 (2014).
- [55] Dominik Schotzau. “Mixed finite element methods for stationary incompressible magneto-hydrodynamics”. In: *Numerische Mathematik* 96.4 (Jan. 2004), pp. 771–800.
- [56] J.N. Shadid et al. “Towards a scalable fully-implicit fully-coupled resistive MHD formulation with stabilized FE methods”. In: *Journal of Computational Physics* 229.20 (Oct. 2010), pp. 7649–7671.
- [57] S. Sivasankaran et al. “Hydro-magnetic combined convection in a lid-driven cavity with sinusoidal boundary conditions on both sidewalls”. In: *International Journal of Heat and Mass Transfer* 54.1-3 (Jan. 2011), pp. 512–525.
- [58] Juan Pablo Trelles and S. Mahnaz Modirkhazeni. “Variational multiscale method for nonequilibrium plasma flows.” In: *Computer Methods in Applied Mechanics and Engineering* 282 (2014), pp. 87–131.
- [59] Müller Ulrich and Bühler Leo. *Magnetofluidynamics in Channels and containers*. Springer, 2010.

Appendix A

Standard function spaces

We denote by $L^2(\Omega)$ the set of all square Lebesgue integrable functions on $\Omega \subset \mathbb{R}^d$ with associated inner product (\cdot, \cdot) and norm $\|\cdot\|$. This extends naturally to vector valued functions, denoted by $\mathbf{L}^2(\Omega)$, where the inner product is given by,

$$(\mathbf{u}, \mathbf{v}) = \sum_{i=1}^d (u_i, v_i). \quad (\text{A.1})$$

The Sobolev norm for $p = 2$ is,

$$\|v\|_m := \left(\sum_{|\alpha|=0}^m \|D^\alpha v\|^2 \right)^{1/2}.$$

where $\alpha = (\alpha_1, \dots, \alpha_m)$ is a multi-index of length m , $|\alpha| = \sum_{i=1}^m \alpha_i$, and

$$D^\alpha v := \frac{\partial^{|\alpha|} v}{\partial x_1^{\alpha_1} \dots \partial x_m^{\alpha_m}},$$

where the partial derivatives are taken in the weak sense. The semi-norm is given by

$$|v|_m := \left(\sum_{|\alpha|=m} \|D^\alpha v\|^2 \right)^{1/2}.$$

Thus, the Hilbert spaces $H^m(\Omega)$ for $m = 0, 1, 2, \dots$ is simply be defined as functions with bounded m -norm,

$$H^m(\Omega) := \{v : \|v\|_m < \infty\}.$$

Appendix A. Standard function spaces

The space $H^0(\Omega)$ is identified with $L^2(\Omega)$. For vector valued functions, the Hilbert space $\mathbf{H}^m(\Omega)$ is defined as,

$$\mathbf{H}^m(\Omega) := \{\mathbf{v} : v_i \in H^m(\Omega), i = 1, \dots, d\}.$$

The norm on $\mathbf{H}^m(\Omega)$ that we will use is

$$\|\mathbf{v}\|_m = \left(\sum_{i=1}^d \|v_i\|_m^2 \right)^{1/2} \quad (\text{A.2})$$

The semi-norm is thus defined by

$$|\mathbf{v}|_m = \left(\sum_{i=1}^d |v_i|_m^2 \right)^{1/2} = \left(\sum_{i=1}^d \int_{\Omega} \|\nabla v_i\|_{\mathbb{R}^d}^2 dx \right)^{1/2} = \left(\int_{\Omega} \|\nabla \mathbf{v}\|_{\mathbb{R}^{d \times d}} dx \right)^{1/2}. \quad (\text{A.3})$$

We introduce the standard continuous Lagrange finite element spaces. Let \mathcal{T}_h be a simplicial decomposition of Ω , where h denotes the maximum diameter of the elements of \mathcal{T}_h . The standard Lagrange space finite element space of order q is then

$$\mathbb{P}_h^q := \{v \in C(\Omega) : \forall K \in \mathcal{T}_h, v|_K \in \mathbb{P}^q(K)\}, \quad (\text{A.4})$$

where $\mathbb{P}^q(K)$ is the space of polynomials of degree at most q defined on the element K .

Appendix B

Vector identities

In this section we have collected all relevant identities to perform the necessary integration by parts arguments for the readers convenience. All functions are assumed to be in $\mathbf{H}^2(\Omega)$.

$$\mathbf{A} \cdot (\mathbf{B} \times \mathbf{C}) = \mathbf{B} \cdot (\mathbf{C} \times \mathbf{A}) = \mathbf{C} \cdot (\mathbf{A} \times \mathbf{B}), \quad (\text{B.1})$$

$$\nabla \cdot (\mathbf{A} \times \mathbf{B}) = \mathbf{B} \cdot (\nabla \times \mathbf{A}) - \mathbf{A} \cdot (\nabla \times \mathbf{B}), \quad (\text{B.2})$$

$$\nabla \cdot [(\nabla \cdot \mathbf{A})\mathbf{B}] = (\nabla \cdot \mathbf{A})(\nabla \cdot \mathbf{B}) + \mathbf{B} \cdot [\nabla(\nabla \cdot \mathbf{A})], \quad (\text{B.3})$$

$$\nabla \cdot (v\mathbf{w}) = v\nabla \cdot \mathbf{w} + \nabla v \cdot \mathbf{w} \quad (\text{B.4})$$

$$\int_{\Omega} \mathbf{A} \cdot (\nabla \times \mathbf{B}) \, dx = \int_{\Omega} \mathbf{B} \cdot (\nabla \times \mathbf{A}) \, dx - \int_{\partial\Omega} \mathbf{B} \cdot (\mathbf{A} \times \mathbf{n}) \, ds, \quad (\text{B.5})$$

$$\int_{\Omega} \mathbf{B} \cdot [\nabla(\nabla \cdot \mathbf{A})] \, dx = - \int_{\Omega} (\nabla \cdot \mathbf{A})(\nabla \cdot \mathbf{B}) \, dx + \int_{\partial\Omega} (\nabla \cdot \mathbf{A})\mathbf{B} \, ds \quad (\text{B.6})$$

$$\int_{\Omega} v\nabla \cdot \mathbf{w} \, dx = - \int_{\Omega} \nabla v \cdot \mathbf{w} \, dx + \int_{\partial\Omega} v\mathbf{w} \cdot \mathbf{n} \, ds. \quad (\text{B.7})$$

One should note that the integral identities (B.5), (B.6) and (B.7) follow from the component-wise identities (B.1)-(B.4) and the divergence theorem. We also make

Appendix B. Vector identities

use of the following inequalities for $\mathbf{u}, \mathbf{v} \in \mathbf{H}^1(\Omega)$,

$$|\mathbf{u} \cdot \mathbf{v}| \leq \|\mathbf{u}\|_{\mathbb{R}^d} \|\mathbf{v}\|_{\mathbb{R}^d}, \quad (\text{B.8a})$$

$$\|\mathbf{u} \times \mathbf{v}\|_{\mathbb{R}^d} \leq \|\mathbf{u}\|_{\mathbb{R}^d} \|\mathbf{v}\|_{\mathbb{R}^d}, \quad (\text{B.8b})$$

$$\|\nabla \times \mathbf{u}\|_{\mathbb{R}^d} \leq \sqrt{2} \|\nabla \mathbf{u}\|_{\mathbb{R}^{d \times d}}, \quad (\text{B.8c})$$

$$|\nabla \cdot \mathbf{u}| \leq \sqrt{3} \|\nabla \mathbf{u}\|_{\mathbb{R}^{d \times d}} \quad (\text{B.8d})$$

$$\|A\mathbf{v}\|_{\mathbb{R}^d} \leq \|A\|_{\mathbb{R}^{d \times d}} \|\mathbf{v}\|_{\mathbb{R}^d}, \quad (\text{B.8e})$$

and finally the equality

$$\|\nabla \mathbf{v}^T\|_{\mathbb{R}^{d \times d}} = \|\nabla \mathbf{v}\|_{\mathbb{R}^{d \times d}}, \quad (\text{B.9})$$

where throughout for $A \in \mathbb{R}^{d \times d}$,

$$\|A\|_{\mathbb{R}^{d \times d}} = \left(\sum_{i=1}^d \sum_{j=1}^d |a_{ij}|^2 \right)^{1/2} \quad (\text{B.10})$$

is the Frobenius norm and thus,

$$\|\nabla \mathbf{v}\|_{\mathbb{R}^{d \times d}} = \left(\sum_{i=1}^d \|\nabla v_i\|_{\mathbb{R}^d}^2 \right)^{1/2}.$$

Appendix C

Useful inequalities

1. The space $\mathbf{H}^1(\Omega)$ embeds continuously in $\mathbf{L}^4(\Omega)$ with constant $\sqrt{\gamma}$. That is, $\mathbf{H}^1(\Omega) \hookrightarrow \mathbf{L}^4(\Omega)$ such that,

$$\|\mathbf{v}\|_{\mathbf{L}^4} \leq \sqrt{\gamma} \|\mathbf{v}\|_{\mathbf{H}^1}. \quad (\text{C.1})$$

2. We have

$$\|\mathbf{u} \cdot \mathbf{v}\|_{L^2} \leq \|\mathbf{u}\|_{\mathbf{L}^4} \|\mathbf{v}\|_{\mathbf{L}^4}. \quad (\text{C.2})$$

This is seen as follow,

$$\begin{aligned} \|\mathbf{u} \cdot \mathbf{v}\|_{L^2} &= \left(\int_{\Omega} (\mathbf{u} \cdot \mathbf{v})^2 dx \right)^{1/2} \leq \left(\int_{\Omega} \|\mathbf{u}\|_{\mathbb{R}^d}^2 \|\mathbf{v}\|_{\mathbb{R}^d}^2 dx \right)^{1/2} \\ &\leq \left(\left(\int_{\Omega} \|\mathbf{u}\|_{\mathbb{R}^{d \times d}}^4 \right)^{1/2} \left(\int_{\Omega} \|\mathbf{v}\|_{\mathbb{R}^d}^4 \right)^{1/2} \right)^{1/2} = \|\mathbf{u}\|_{\mathbf{L}^4} \|\mathbf{v}\|_{\mathbf{L}^4}. \end{aligned}$$

3. We have,

$$\|\mathbf{u} \times \mathbf{v}\|_{L^2} \leq \|\mathbf{u}\|_{\mathbf{L}^4} \|\mathbf{v}\|_{\mathbf{L}^4} \quad (\text{C.3})$$

Appendix C. Useful inequalities

as shown below,

$$\begin{aligned} \|\mathbf{u} \times \mathbf{v}\|_{\mathbf{L}^2} &= \left(\int_{\Omega} \|\mathbf{u} \times \mathbf{v}\|_{\mathbb{R}^d}^2 dx \right)^{1/2} \stackrel{\text{(B.8b)}}{\leq} \left(\int_{\Omega} \|\mathbf{u}\|_{\mathbb{R}^d}^2 \|\mathbf{v}\|_{\mathbb{R}^d}^2 dx \right)^{1/2} \\ &\leq \left(\left(\int_{\Omega} \|\mathbf{u}\|_{\mathbb{R}^{d \times d}}^4 \right)^{1/2} \left(\int_{\Omega} \|\mathbf{v}\|_{\mathbb{R}^d}^4 \right)^{1/2} \right)^{1/2} = \|\mathbf{u}\|_{\mathbf{L}^4} \|\mathbf{v}\|_{\mathbf{L}^4}. \end{aligned}$$

4. The Cauchy-Schwarz inequality for $[a, b], [c, d] \in \mathbb{R}^2$,

$$ac + bd = [a, b] [c, d]^T \leq \sqrt{a^2 + c^2} \sqrt{b^2 + d^2}, \quad (\text{C.4})$$

5. The following inequality follows from the Poincaré inequality is,

$$\|\nabla \mathbf{v}\|_0^2 \geq k_1 \|\mathbf{v}\|_1^2, \quad \forall \mathbf{v} \in \mathbf{H}_0^1(\Omega). \quad (\text{C.5})$$

6. For $x, y \in \mathbb{R}$,

$$-xy \geq -\frac{1}{2}(x^2 + y^2), \quad (\text{C.6})$$

We also need the following propositions,

Proposition C.0.1. *Let $\mathbf{u}, \mathbf{v}, \mathbf{w} \in \mathbf{H}^1(\Omega)$. Then there holds*

$$\int_{\Omega} \mathbf{u}^T (\nabla \mathbf{v}) \mathbf{w} dx \leq \|\mathbf{u}\|_{\mathbf{L}^4} \|\mathbf{w}\|_{\mathbf{L}^4} \|\mathbf{v}\|_1. \quad (\text{C.7})$$

Proof. We will work with the integrand first. To this end, we have that

$$\begin{aligned} \mathbf{u}^T (\nabla \mathbf{v}) \mathbf{w} &= \sum_{i=1}^d u_i \mathbf{w}^T \nabla v_i \leq \sum_{i=1}^d |u_i| \|\mathbf{w}\|_{\mathbb{R}^d} \|\nabla v_i\|_{\mathbb{R}^d} = \|\mathbf{w}\|_{\mathbb{R}^d} \sum_{i=1}^d |u_i| \|\nabla v_i\|_{\mathbb{R}^d} \\ &\leq \|\mathbf{w}\|_{\mathbb{R}^d} \left(\sum_{i=1}^d |u_i|^2 \right)^{1/2} \left(\sum_{i=1}^d \|\nabla v_i\|_{\mathbb{R}^d}^2 \right)^{1/2} \stackrel{\text{(B.10)}}{=} \|\mathbf{w}\|_{\mathbb{R}^d} \|\mathbf{u}\|_{\mathbb{R}^d} \|\nabla \mathbf{v}\|_{\mathbb{R}^{d \times d}}. \end{aligned}$$

Now we integrate,

$$\begin{aligned} &\int_{\Omega} |\mathbf{w}\|_{\mathbb{R}^d} \|\mathbf{u}\|_{\mathbb{R}^d} \|\nabla \mathbf{v}\|_{\mathbb{R}^{d \times d}} dx \\ &\leq \left(\int_{\Omega} \|\mathbf{u}\|_{\mathbb{R}^d}^2 \|\mathbf{w}\|_{\mathbb{R}^d}^2 dx \right)^{1/2} \left(\int_{\Omega} \|\nabla \mathbf{v}\|_{\mathbb{R}^{d \times d}}^2 \right)^{1/2} \\ &\leq \left(\int_{\Omega} \|\mathbf{u}\|_{\mathbb{R}^d}^4 dx \right)^{1/4} \left(\int_{\Omega} \|\mathbf{w}\|_{\mathbb{R}^d}^4 dx \right)^{1/4} \left(\int_{\Omega} \|\nabla \mathbf{v}\|_{\mathbb{R}^{d \times d}}^2 dx \right)^{1/2} \\ &= \|\mathbf{u}\|_{\mathbf{L}^4} \|\mathbf{w}\|_{\mathbf{L}^4} \|\mathbf{v}\|_1 \leq \|\mathbf{u}\|_{\mathbf{L}^4} \|\mathbf{w}\|_{\mathbf{L}^4} \|\mathbf{v}\|_1. \end{aligned}$$

Appendix C. Useful inequalities

□